Photochemical oxidative addition of germane and diphenylgermane to ruthenium dihydride complexes

David P. Dickinson,[†] Simon W. Evans,[†] Mary Grellier,[‡] Hannah Kendall,[†] Robin N. Perutz,[†*] Barbara Procacci,[†*] Sylviane Sabo-Etienne,[‡] Katharine A. Smart,[‡] and Adrian C. Whitwood[†]

[†] Department of Chemistry, University of York, York, YO10 5DD, UK.

[‡] LCC-CNRS, Université de Toulouse, CNRS, UPS, 31077 Toulouse, France

ABSTRACT: Photochemical reactions of germane and diphenylgermane with $Ru(PP)_2H_2$ (PP = $R_2PCH_2CH_2PR_2$ or DuPhos, R = Ph dppe, R = Et depe, R = Me dmpe) are reported. Reaction with GeH_4 generates a mixture of *cis*- and *trans*-isomers of $Ru(PP)_2(GeH_3)H$ except for the DuPhos complex which yields the product only in the *cis* form. *In-situ* laser photolysis (355 nm) demonstrates that the initial product is the *cis*-isomer that undergoes thermal isomerization to the *trans*-isomer. The complex *cis*-$[Ru(dppe)_2(GeH_3)H]$ crystallizes selectively, allowing determination of its X-ray structure as a germyl hydride with a long Ru–H···Ge separation of 2.64(3) Å indicating that no residual interaction between the RuH and Ge is present. DFT calculations are also consistent with full oxidative addition. The structure of *cis*-$[Ru(DuPhos)_2(GeH_3)H]$ reveals significant distortion from an octahedral geometry. The major species in the crystal (95%) exhibits a structure with a Ru–H···Ge distance of 2.42(5) Å suggesting negligible interaction between these centers. DFT calculations of the structure are consistent with the experimental determination. The reactions of $Ru(PP)_2H_2$ with diphenylgermane yield *cis*-$[Ru(PP)_2(GePh_2H)H]$ exclusively for PP = dmpe and depe, while the *cis*-isomer is dominant in the case of dppe. A photochemical competition reaction between $Ru(dppe)_2(H)_2$ and the two substrates Ph_2SiH_2 and Ph_2GeH_2 results in both Si–H and Ge–H oxidative addition activation with a kinetic preference (0.18:1) for the germyl hydride product. Thermal conversion of $Ru(dppe)_2(SiPh_2H)H$ to $Ru(dppe)_2(GePh_2H)H$ is observed on heating.

INTRODUCTION

It is now well recognized that the organosilicon-based ligands bond to transition metals in a wide variety of ways including metal-silicon single and multiple bonds, and M–H–Si three centre bonding motifs.[1-3] The success with organosilicon chemistry is driven both by the importance of silicon in catalysis and by the availability of numerous precursors. Our knowledge of the corresponding germanium chemistry is not commensurate with its potential – it is limited by a lack of readily available precursors and a lack of known catalytic applications. In a previous paper, we addressed the differences between silicon and germanium in forming Ru=E double bonds and in forming Ru–H–E interactions (E = Si or Ge).[4] We now use GeH_4 to make ruthenium germyl hydride complexes by oxidative addition and compare the reactivity of different $Ru(PP)_2H_2$ (PP = $R_2PCH_2CH_2PR_2$, R = Me, Et, Ph) complexes toward germane and diphenylgermane.

Comparisons of SiH_4 and GeH_4 show that the bond dissociation energy of SiH_4 is greater than that of GeH_4 (383.7 ± 2.1 and 348.9 ± 8.4 kJ mol^{-1}, respectively)[5] and the vertical ionization energy measured from the photoelectron spectrum is greater (12.36 and 11.98 eV, respectively).[6] The IR-active t_2 E-H stretching vibration is also higher for silane than for germane (2183 and 2114 cm^{-1}, respectively).[7] The Ge–H bond dissociation energy of Ph_2GeH_2 is reported to be 333 ± 3 kJ mol^{-1}, about 5% lower than that of germane[8a] (see also recent review of thermochemistry of Ge compounds)[8b].

Most studies of oxidative addition of organogermanium compounds at transition metals involve Ph_3GeH, Ph_2GeH_2, Et_3GeH, and Et_2GeH_2. Only a few address the simplest germane, GeH_4, although germane is considerably more benign than silane.[9] In pioneering work, the thermal reactions of $Ir(PEt_3)_2X(CO)$ (X = Cl, I) with SiH_4 and GeH_4 were shown to afford oxidative addition products $IrH(EH_3)(PEt_3)_2(X)(CO)$ (E = Si, Ge).[10] In 2015, the reaction of Vaska's complex $Ir(PPh_3)_2(CO)Cl$ with SiH_4 and GeH_4 was examined.[11] A combination of X-ray structure analysis of the SiH_4 oxidative addition product and NMR spectroscopy led to assignments of these products and reassignment of the geometries of the earlier PEt_3

complexes (Scheme 1). No crystal structure was obtained for the Ir-germyl complexes and neither study provided evidence of rearrangement of isomers.

Scheme 1. Products of reaction of $Ir(PR_3)_2(CO)Cl$ with SiH_4 and GeH_4 (R = Ph, Et)[10,11]

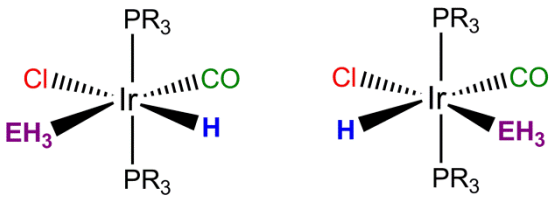

Cis oxidative addition of EH_4 (E = Si, Ge)
E = Ge, formation of both **A** and **B**
E = Si, formation of **B**

Comparison of the reactivity of agostic $Mo(CO)(PP)_2$ (PP = $R_2PCH_2CH_2PR_2$; R = Ph dppe, R = Et depe) toward silane and germane revealed the η^2-coordination product $Mo(CO)(PP)_2(\eta^2\text{-}SiH_4)$ for R = Ph, ^{i}Bu, whereas a mixture of oxidative addition and η^2-SiH_4 products was obtained for R = Et.[12,13] Formation of the η^2-GeH_4 complex $Mo(CO)(dppe)_2(\eta^2\text{-}GeH_4)$ was demonstrated by IR and NMR spectroscopy, while the analogue with R = Et was shown to adopt a germyl hydride structure $Mo(CO)(depe)_2(GeH_3)H$.[13] Further studies (see below) established a general trend in which oxidative addition is favored thermodynamically over η^2-coordination in the order Ge–H > Si–H ≈ H–H >> C–H for these Mo complexes. DFT calculations showed that the oxidative addition of EH_4 to $Mo(CO)(H_2PCH_2CH_2PH_2)_2$ is more favorable by ca. 5 kcal mol^{-1} for E = Ge than for E = Si.[13] A DFT study of the coordination of GeH_4 to $RuH_2(\eta^2\text{-}H_2)_2(PH_3)_2$ found that the oxidative addition of germane was marginally more favorable than the η^2-GeH coordination in $RuH_2(\eta^2\text{-}H_2)(\eta^2\text{-}H\text{–}GeH_3)(PH_3)_2$. Notably, silane chemistry presented the reverse situation. The binding energy of SiH_4 was more favorable than that of GeH_4.[14]

Phenyl germanes, $PhGeH_3$, Ph_2GeH_2, Ph_3GeH are the commonest organogermanes to be employed with transition metals yielding several examples of mononuclear[15-17] and di/polynuclear oxidative addition products[15,16,18] Addition of $PhGeH_3$ across a metal-metal bond has also been documented.[19] The reaction of $Pt(PCy_3)_2$ with diphenylgermane illustrates initial formation of the *cis*-oxidative addition product followed by isomerization to the more stable *trans*-product.[16] The reaction of $[Mo(CO)(depe)_2]_2(\mu\text{-}N_2)$ with Ph_2GeH_2 generates an equilibrium mixture of the η^2-GeH product and oxidative addition product in solution, whereas the corresponding reaction with $PhGeH_3$ forms the oxidative addition product. The dppe complex $Mo(CO)(dppe)_2$ does not react with Ph_2GeH_2 but reacts with $PhGeH_3$ to form an equilibrium mixture of the two types of product. The general shift toward oxidative addition for the organogermanes when compared to the organosilanes follows the same pattern as mentioned above with similar bond energy trends.[13] The reaction of Ph_3GeH with $[(MeCp)Mn(CO)_2]$ formed on irradiation of $(MeCp)Mn(CO)_3$ yields an η^2-GeH product analogous to the product formed with Ph_3SiH.[20,21] The reaction of Ph_3GeH with $RuH_2(\eta^2\text{-}H_2)_2(PCy_3)_2$ yielded an η^2-GeH complex, $RuH_2(\eta^2\text{-}H_2)(\eta^2\text{-}HGePh_3)(PCy_3)_2$ identified by NMR spectroscopy; the silane analogue behaves similarly.[22,23]

When more than two coordination sites become available for interaction with the incoming substituted germane, new reactivity patterns emerge that go beyond oxidative addition/η^2-coordination. Thus, reaction of Cp*Mo(dmpe)(η^3-benzyl) with diphenylgermane yields a germylene hydride complex $Cp^*Mo(dmpe)(H)(=GePh_2)$ while reaction of $Cp^*Ru(P^iPr_3)(OTf)$ with dimesitylgermane gives the germylene dihydride complex $[Cp^*Ru(P^iPr_3)(H)_2(GeMes_2)](OTf)$.[24,25] A critical feature of the $Mo(H)(=EPh_2)$ complexes relates to the question of three-centre Mo···H···E interactions which are present for E = Si, but absent for E = Ge. However, they are present for both Si and Ge in the $Mo{=}EEt_2$ analogues.[26,24] A cyclometalated $Ru(SiP^{Ph}_3)$ complex (SiP^{Ph}_3 is a tripodal phosphine) has been shown to react with diphenylsilane or diphenylgermane to form $HRu{=}EPh_2$ complexes.[27] The reaction of $Ru(H)_2(\eta^2\text{-}H_2)_2(PCy_3)_2$ with diphenylgermane yielded a ruthenium germylene

dihydrogen complex $Ru(H)_2(\eta^2\text{-}H_2)(=GePh_2)(PCy_3)_2$. An intermediate in the reaction was detected that could be formulated either as $Ru\text{-}GePh_2H$ or as a $Ru(\eta^2\text{-}GeHPh_2H)$ complex.[4] In contrast, the dinuclear SiH_4 complex $[(PR_3)_2(H)_2Ru(SiH_4)Ru(H)_2(PR_3)_2]_2$ was obtained upon reaction of the same bis(dihydrogen) precursor with diphenylsilane as a result of redistribution of the substituents in the Ph_2SiH_2 reactant.[28,29] A further class of reaction is illustrated by the addition of each of the phenylgermanes across a Pd=C bond in $[Pd(PCP)(PR_3)]^+$ forming a Pd-Ge bond and a C–H bond. In contrast, the corresponding silanes generate mixtures containing some of the analogous products and some with the addition reversed, forming a Pd-H bond and a C–Si bond.[30] A remarkable reaction occurs between *cis*-$PdMe_2(PMe_3)_2$ and diphenylgermane in the presence of ^{t}BuNC yielding a complex with a Pd_2Ge_4 core with close Ge···Ge interactions. Further reaction with depe releases the digermane $HPh_2Ge–GePh_2H$ and forms Pd–Ge complexes; heating this mixture gives a trigermane $HPh_2Ge–GePh_2–GePh_2H$.[31]

The balance between η^2-GeH and oxidative addition products has also been analyzed for photoreactions of molybdenum and tungsten carbonyls with Et_3GeH and Et_2GeH_2.[32-35] A more recent study addresses analogous comparisons for the reactions of Et_3EH (E = Si, Ge) with rhodium and iridium diiminato complexes to form species of the type $M(diiminato)(EEt_3)_2(H)_2$.[36]

The research reported here builds on our studies of the steady-state and time-resolved photochemistry of ruthenium dihydride complexes in the presence of other substrates.[37-40] All these complexes undergo photochemical reductive elimination of H_2 to form transient 16-electron $[Ru(PP)_2]$ (PP = $R_2PCH_2CH_2PR_2$) intermediates that are highly reactive toward E–H bonds. In this paper, we exploit the relatively benign nature of GeH_4 compared to SiH_4 to study an unsubstituted substrate which could result in mononuclear or dinuclear products and could form germyl or germylene products. We also report investigations of the reactivity of Ph_2GeH_2 in the presence of $Ru(PP)_2H_2$, designed to compare to our earlier work with substituted silanes. Both the *cis*- and *trans*-forms of reactants and products are observed enabling us to explore

isomerization processes. The initial studies were made with $Ru(dppe)_2H_2$, **1Ph**, but we extended the study to dmpe, depe and DuPhos analogues in order to compare the effect of different diphosphines (Scheme 2).

Scheme 2. Reactions and complexes under study

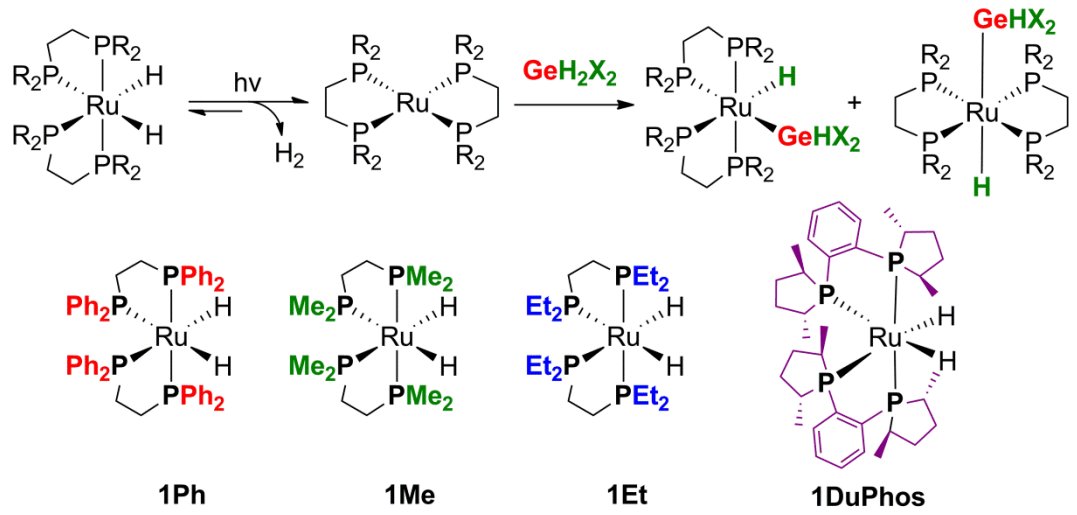

GeH_2X_2 = GeH_4, Ph_2GeH_2

RESULTS AND DISCUSSION

The complex $Ru(dppe)_2H_2$ **1Ph** is characterized by its hydride signal in the ^1H NMR spectrum centred at δ –8.30 which arises from the overlap of a second order multiplet for the *cis*-isomer and a quintet for the *trans*-isomer (See SI). The $^1H\{^{31}P\}$ NMR separates the two singlets for the *cis*- at δ –8.30 and *trans*-isomers at –8.10 in a 20:1 ratio, respectively. In the $^{31}P\{^1H\}$ NMR spectrum, the *trans*-complex appears as a singlet at δ 83.9 whereas the *cis*-complex exhibits two triplets at δ 79.5 and 65.7 ($^2J_{PP}$ = 15.0) (See SI). Germane shows a singlet at δ 3.05 with Ge satellites (J_{GeH} = 97.3 Hz). The concentration of GeH_4 present in solution is limited by its poor solubility in benzene. In typical reactions, Ru was in excess before irradiation and photolysis was stopped intermittently to replenish germane by condensation.

Broadband steady state photolysis of 1Ph with GeH_4. The complex **1Ph** does not react thermally at room temperature in the presence of germane gas, but does react upon irradiation (λ > 290 nm, 3.5 h, room temperature, 100% NMR conversion) to yield new products. The ^{1}H NMR spectrum shows two new hydride resonances; a doublet of apparent quartets at δ –8.92 ($^2J_{HP(trans)}$ = 70, $^2J_{HP(cis)}$ = 20 Hz), indicative of a *cis*-geometry around the metal centre and a quintet at δ –8.48 ($^2J_{HP}$ = 19 Hz) suggesting a *trans*-geometry (Figure 1a). The ^{1}H NMR spectrum also shows two new resonances in the region characteristic for germyl protons: quintets at δ 2.66 ($^3J_{HP}$ = 6 Hz, *cis*) and δ 2.50 ($^3J_{HP}$ = 3 Hz, *trans*) (Figure 1a). Upon ^{31}P decoupling both hydride and germyl resonances simplify to singlets with a *cis:trans* ratio of 1.15:1 (Figure 1b). The ^{31}P{^{1}H} NMR spectrum also shows the clean formation of two new products. The *cis*-species contains phosphorus atoms which are magnetically and chemically inequivalent, leading to an ABQX spin system. The resonances for the mutually *trans*-phosphorus nuclei (AB) overlap, affording a multiplet at δ 72.8; whereas the two remaining resonances (Q and X) are observed at δ 68.2 and 52.2 (See SI). The four resonances show mutual cross peaks in ^{31}P-^{31}P COSY 2D spectroscopy confirming that they belong to the same species; the same resonances couple to the hydride at δ –8.92 and to the germyl peak at δ 2.66 in the ^{1}H-^{31}P HMQC experiment. A singlet is observed for the four equivalent phosphorus nuclei of the *trans*-species at δ 72.2 with cross peaks to the hydride and germyl peaks in the ^{1}H-^{31}P HMQC spectrum (See SI). A more detailed NMR characterization is given in Table 1. This product was also characterized by LIFDI and high resolution EI mass spectrometry. On the basis of these results, we assign the two products as *cis*- and *trans*-Ru(dppe)$_2$(GeH_3)H, ***cis*-2Ph** and ***trans*-2Ph** respectively, formed from oxidative addition of germane to the Ru(0) square planar intermediate.[38]

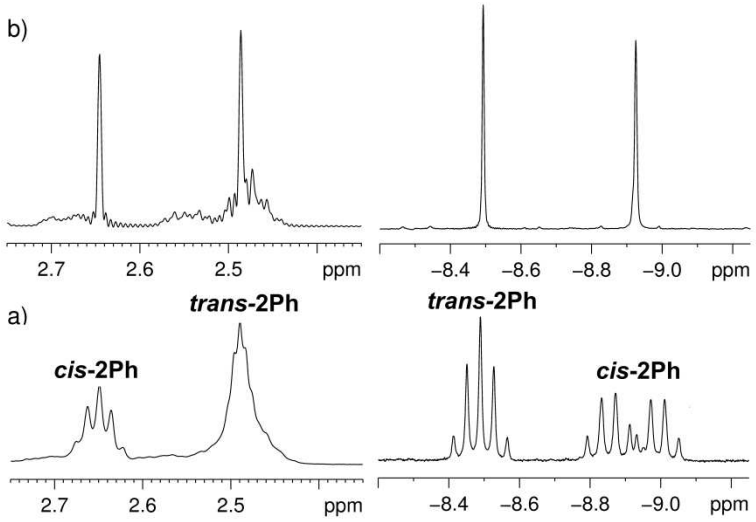

Figure 1. (a) ^{1}H NMR spectrum and (b) $^{1}H\{^{31}P\}$ NMR spectrum of the products of the photochemical reaction of **1Ph** with germane in C_6D_6 in the germyl region (left) and hydride region (right).

Crystals suitable for X-ray analysis were obtained by crystallization of a concentrated benzene solution of a mixture of ***cis*-2Ph** and ***trans*-2Ph** layered with hexane; the structure revealed ***cis*-2Ph** as the dominant complex in the crystal (occupancy 0.9193(15)) with small amounts of the *trans*-germyl species (0.0546(14)) ***trans*-2Ph** and *cis*-digermyl *cis*-$[Ru(dppe)_2(GeH_2GeH_3)H]$ (0.0226(7)) complex (See SI, this product was not detected by NMR spectroscopy). For the major component ***cis*-2Ph**, the germyl hydrogens were placed using a riding model with the Ge-H bond length restrained to be 1.53 Å. The ruthenium hydride was located by difference map and allowed to refine. The minor components, ***trans*-2Ph** and the digermyl complex were present in such small quantities that for the former, only the phosphorus, germanium and ruthenium atoms could be modelled and for the latter, all atoms apart from the digermyl group were assumed to be coincident with those of the ***cis*-2Ph**. For both of these minor components, the germyl hydrogens were added as above. Bond lengths and angles for the major species ***cis*-2Ph** are listed in Table 2. Further crystallographic data are given in the SI. The Ru–Ge and Ru–Hydride (H1) bond lengths of the complex ***cis*-2Ph**

are determined as 2.5039(4) Å and 1.69(3) Å, respectively (Figure 2). The Ge···H1 separation of 2.64(3) Å is much longer than the bound Ge–H distance of 1.53 Å showing that the activation of Ge–H by the metal complex has proceeded to complete oxidative addition. For comparison, the Ge–H bond lengths in germane and digermane are 1.527(3) Å (vibration-rotation spectroscopy) and 1.541(6) Å (gas electron diffraction), respectively,[41,42] while η^2-Ge–H interactions range from 1.65 to 2.1 Å according to either X-ray or DFT.[13,15,16,24,35] A value of the Ge···H(1) separation greater than 2.30 Å is consistent with full oxidative addition.[43] The hydride ligand shows the greatest *trans*-influence reflected in the longer Ru–P4 distance of 2.3765(18) Å compared to that of Ru–P2 at 2.3351(8) Å which is *trans* to GeH_3. There is only one reported structure with a Ru–GeH_3 moiety determined by X-ray crystallography; the complex $Ru(GeH_3)(\eta^5\text{-}C_5H_5)(PPh_3)\{P(OMe)_3\}$ showed a Ru–Ge bond length of 2.4421(9) Å and an average Ge–H bond distance of 1.50(6) Å.[44] There are only a few other transition metal-GeH_3 complexes in the crystallographic database.[45-48] Additionally, there are gas-phase electron diffraction structures of $M(GeH_3)(CO)_5$ (M = Mn, Re) and $Co(GeH_3)(CO)_4$.[49-51] The presence of the ***trans*-2Ph** species at 5.5%, compared to 91.9% for ***cis*-2Ph** is not representative of the 1:1.15 ratio observed in solution. This implies that the complex ***cis*-2Ph** crystallizes preferentially. We redissolved some crystals and measured NMR spectra which showed that both *cis* and *trans* isomers were present. We have also demonstrated equilibration between *cis* and *trans* isomers independently (see below).

Table 1. NMR data for the products of photo-reaction of 1Ph, 1Me, 1Et, and 1DuPhos with GeH_4 in C_6D_6 δ / mult / *J* (Hz)

Product	^{1}H NMR GeH[a]	^{1}H NMR RuH	^{31}P NMR P_{AB}	^{31}P NMR P_X[b]	^{31}P NMR P_Q[b]
***cis*-2Ph**	2.66 (app quin, $^3J_{HP}$ = 6)	–8.92 (app dq, J_{HP} = 70, 20)	72.04 (m)	67.5 (m)	51.4 (J_{QA} = 23, J_{QX} = 11)
***cis*-2Me**	3.11 (m)	–10.09 (app dq, J_{HP} = 72, 23)	43.4 (AB quart of dd, $^2J_{AB}$ = 250, $^2J_{AX}$ = 25, $^2J_{AQ}$ = 25, $^2J_{BX}$ = 30, $^2J_{BQ}$ = 17)	41.8 (m)	29.9 (J_{QA} = 23, J_{QX} = 16)
***cis*-2Et**	2.90 (quin, $^3J_{HP}$ = 6)	–10.74 (app dq, J_{HP} = 71, 22)	67.7 (AB quart of dd, J_{AB} = 237, J_{AQ}, J_{AX} = 22)	66.95 (m)	58.3 (dd, J_{QA} = 22, J_{QX} = 17)
***cis*-2DuPhos**[c]	3.75 (quin, $^3J_{HP}$ = 5)	–9.36 (ddt, $^2J_{HP}$: $J_{HPtrans}$ = 68, J_{HPcis} = 24, J_{HPcis} = 17)	99.2 (AB quart of dd, J_{AB} = 227, J_{AX} = 30, J_{AQ} = 21, J_{BX}, J_{BQ} = 25)	79.0 (dd, J_{XA} = 30, J_{XQ} = 22	58.3 (m)
***trans*-2Ph**	2.50 (app quin, $^3J_{HP}$ = 3)	–8.48 (quin, J_{HP} = 19)	72.20 (s)		
***trans*-2Me**	2.71 (quin) $^3J_{HP}$ = 4.6	–11.20 (quin,J_{HP} = 21.0)	44.2 (s)		
***trans*-2Et**	2.88 (quin, $^3J_{HP}$ = 4)	–11.29 (quin, $^2J_{HP}$ = 20)	66.27 (s)		

[a] GeH_4 δ 3.05
[b] P_x lies *trans* to Ge, P_Q lies *trans* to H
[c] *trans*-isomer not observed

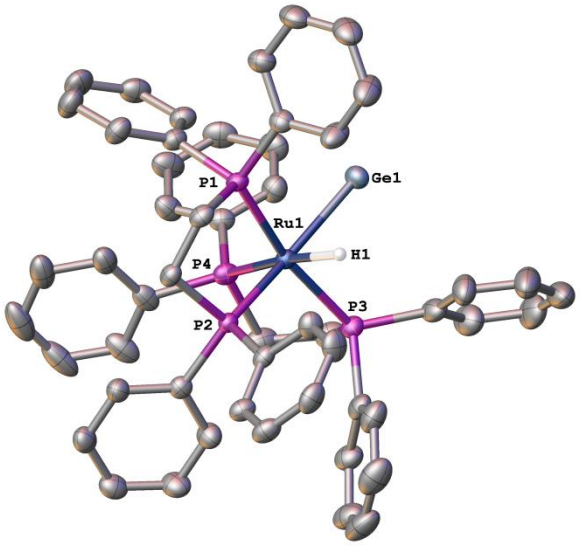

Figure 2. Molecular structure of *cis*-[Ru(dppe)$_2$(GeH$_3$)H]·0.5C$_6$H$_6$, ***cis*-2Ph·0.5C$_6$H$_6$**. Hydrogen atoms, with the exception of the hydride ligand, are not shown. Anisotropic displacement parameters are shown at the 50% level. The minor components in the crystal are not shown.

Table 2. X-ray and DFT bond lengths (Å) and angles (º) for *cis*-Ru(dppe)$_2$(GeH$_3$)H·0.5C$_6$H$_6$, *cis*-2Ph·C$_6$H$_6$ and *cis*-Ru(DuPHOS)$_2$(GeH$_3$)H, *cis*-2DuPhos.[a]

Atoms	***cis*-2Ph**	***cis*-2Ph (DFT)**	***cis*-2DuPhos**	***cis*-2DuPhos (DFT)**
Ru–Ge1	2.5039(4)	2.516	2.4673(6)	2.494
Ru1–P1	2.3156(9)	2.296	2.2995(12)	2.291
Ru1–P2	2.3351(8)	2.317	2.3012(12)	2.292
Ru1–P3	2.3203(8)	2.299	2.3150(12)	2.296
Ru1–P4	2.3765(18)	2.349	2.3485(12)	2.347
Ru1–H1	1.69(3)	1.617	1.57(5)	1.615
Ge···H1	2.64(3)	2.730	2.42(5)	2.421

P1–Ru1–Ge1	85.17(2)	85.53	91.11(3)	91.28
P1–Ru1–P2	83.74(3)	84.36	81.73(4)	82.95
P1–Ru1–P3	168.57(3)	167.42	175.87(5)	176.49
P1–Ru1–P4	104.77(4)	104.71	95.97(4)	95.47
P2–Ru1–Ge1	161.90(2)	164.77	147.03(4)	150.25
P2–Ru1–P4	95.82(5)	94.56	102.38(4)	100.38
P3–Ru1–Ge1	86.23(2)	84.54	92.02(3)	91.20
P2–Ru1–P3	102.59(3)	103.72	97.04(4)	96.08
P3–Ru1–P4	84.23(4)	84.49	80.41(4)	81.37
P4–Ru1–Ge1	100.83(4)	99.01	110.38(3)	109.24
H1-Ru1-Ge1	75.2(11)	79.4	69.8(19)	68.38

[a] The listings are for the major species only

The energies, structures and vibrational frequencies of ***cis*-2Ph** and ***trans*-2Ph** were calculated by DFT methods. The structure of ***cis*-2Ph** matches the X-ray structure well; the identification of ***cis*-2-Ph** as an oxidative addition product is supported by the DFT calculations which yield a Ge···H separation of 2.730 Å. According to DFT, ***cis*-2Ph** lies 11.5 kJ mol^{-1} (ΔG) lower in energy than ***trans*-2Ph**, although experiments show the *trans*-isomer to be lower in energy (see below). The relative energies were unchanged on inclusion of solvent.

Change of the phosphine (PP) ligand: effects on reaction with GeH_4. A series of complexes analogous to **1Ph** were prepared in order to explore the changes in reactivity introduced by phosphine ligands with different electronic and steric properties from those of dppe. The complexes investigated, **1Me**, **1Et**, and **1DuPhos** are shown in Scheme 2 and their

NMR characteristics are given in the SI. None of the precursors react thermally with GeH_4 at room temperature. NMR data for the photoproducts are listed in Table 1.

$Ru(dmpe)_2H_2$, **1Me** reacts with GeH_4 photochemically to yield new species ($\lambda > 290$ nm, 2.5 h, room temperature, 100% NMR conversion). The products ***cis*-2Me** and ***trans*-2Me** were readily identified and characterized by comparison to ***cis*-2Ph** and ***trans*-2Ph**. Upon ^{31}P decoupling both hydride resonances simplified to singlets, and gave a ratio of ***cis*-2Me**:***trans*-2Me** equal to 1.27:1.

$Ru(depe)_2H_2$, **1Et** converts by photolysis with GeH_4 ($\lambda > 290$ nm, 3 h, room temperature, 100% NMR conversion) to a mixture of *cis*- and *trans*-species ***cis*-2Et** and ***trans*-2Et**, respectively. The ratio between the two isomers, given by integration of the hydride resonances when ^{31}P decoupled, was found to be 1 cis :0.7 trans.

In line with the previous experiments, $Ru(DuPhos)_2H_2$, **1DuPhos** reacts photochemically in the presence of GeH_4 but **DuPhos** generated only the *cis*-isomer ***cis*-2DuPhos**. A crystal structure of ***cis*-2DuPhos** was obtained by X-ray diffraction (Figure 3). The structure was modeled with the germanium in two positions; the major component (population 0.9522(14)) corresponds to a ruthenium germyl hydride. The ruthenium hydride was located by difference map and allowed to refine. The Ge–H positions were set with a riding model using a fixed bond length of 1.53 Å. The minor component (population 0.0478(14)) was distinguished by the position of germanium, while other atoms are assumed to be coincident with those in the major component. The hydrogens on the germanium of the minor component were not modeled. Relevant bond lengths and angles for the major component are listed in Table 2. The Ru–Ge and Ru–P bond lengths are consistently slightly shorter than those of ***cis*-2Ph** and once more, the hydride shows the strongest *trans*-influence. The angles P2–Ru–Ge and P4–Ru–Ge (147.03(4)º and 110.38(3)º, respectively) are distorted away from the ideal octahedron as was observed for the analogues *cis*-$[Ru(DuPhos)_2(SiEt_2H)H]$ and *cis*-$[Ru(DuPhos)(SiPhH_2)H]$.[39] The ruthenium-bound hydride was located with a Ru–H distance of 1.57(5) Å. The Ge···hydride distance is 2.42(5) Å compared with 2.64(3) Å for **cis-2Ph**. DFT

calculations are in excellent agreement and confirm the absence of any interaction between the germanium center and the hydride (Ge···H 2.421 Å). The minor component is tentatively assigned as an η^2-GeH_4 complex on the basis of the off-axis position of Ge. The Ru–Ge distances in **cis-2Ph**, **cis-2DuPhos** of 2.5039(4) and 2.4673(6) Å, respectively, are consistent with that in the only other published structure of a Ru-GeH_3 complex, Ru(GeH_3)(η^5-C_5H_5)(PPh_3){$P(OMe)_3$} (2.4421(9) Å).[44]

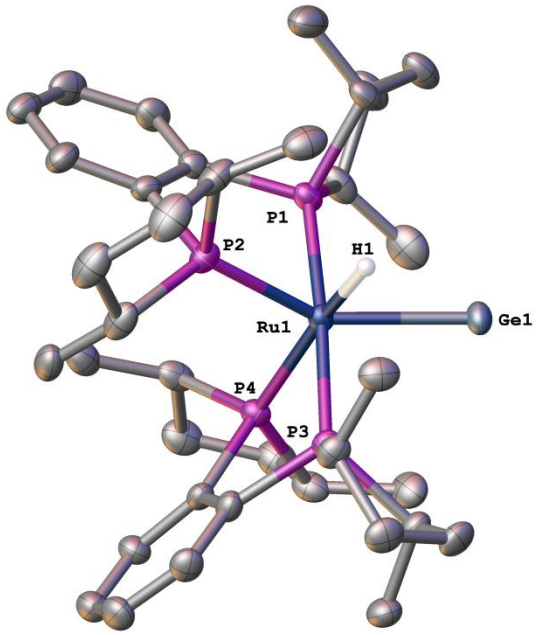

Figure 3. Crystal structure of *cis*-[Ru($DuPhos)_2$(GeH_3)H], ***cis*-2DuPhos**. Hydrogen atoms, with the exception of the Ru-hydride ligand are not shown. Anisotropic displacement parameters are shown at the 50% level. The minor component is illustrated in the SI.

***In-situ* monochromatic photolysis of 1Ph with GeH_4.** The reaction of **1Ph** (optically dilute solution in C_6D_6) with GeH_4 was followed by *in-situ* photolysis at 355 nm within an NMR probe at room temperature. The sample was photolyzed with sets of laser shots so that the formation of the product and/or any transient species could be monitored. The *cis*- and *trans*-starting material hydride peaks are shown at δ –8.34 and –8.17, respectively (Figure 4a). The detection of a new species was achieved after 75 laser shots (laser frequency 10 Hz) and the

compounds were identified by their hydride resonances (δ –8.50 and –8.93) as ***cis*-2Ph** and ***trans*-2Ph** (Figure 4). The ***cis*-2Ph** product forms initially whereas ***trans*-2Ph** appears on a longer timescale. This feature supports the formation of the ***trans*-2Ph** product *via* the ***cis*-2Ph** species either through secondary photoisomerization or through thermal equilibration. Interestingly, the production of ***cis*-2Ph** and ***trans*-2Ph** reaches a plateau with increasing photolysis time, perhaps due to back reaction of H_2 in solution generated by reductive elimination from **1Ph**. Since there is only a small quantity of GeH_4 present in solution due to its poor solubility, the H_2 produced by photolysis becomes a competing substrate under these reaction conditions.

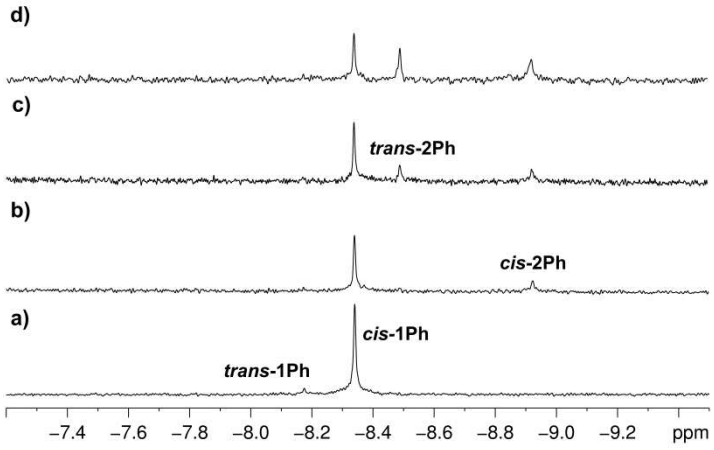

Figure 4. $^{1}H\{^{31}P\}$ NMR spectra of the *in-situ* photolysis of **1Ph** with GeH_4 in C_6D_6 after (a) 0, (b) 75, (c) 155 and (d) 325 laser shots at 355 nm.

Low temperature photolysis of 1Ph in the presence of GeH_4. In order to monitor the thermal equilibration of the ***cis*-2Ph** and ***trans*-2Ph** isomers, the photochemical reaction of a solution of **1Ph** with GeH_4 in tol-d_8 was conducted at low temperature (195 K). Following 3 h photolysis at 195 K with a broadband source, the sample was analyzed by $^{31}P\{^{1}H\}$ NMR spectroscopy with the spectrometer set at 270 K. The spectrum showed the ***cis*-2Ph** product almost exclusively identified by its ABQX spin system, with very little ***trans*-2Ph**, as shown by

the small singlet at δ 73.1 in Figure 5a. The sample was left in the spectrometer for 5 min (Figure 5b) resulting in a significant increase in intensity of the singlet at δ 73.1. A further increase occurred on raising the temperature of the NMR spectrometer to 280 K (Figure 5c). When the spectrometer was warmed to room temperature (295 K), the resonance for ***trans*-2Ph** increased and integration gave the expected *cis:trans* ratio of 1.15:1 as observed in the earlier experiments at room temperature (Figure 5d). These findings provide evidence that ***cis*-2Ph** is the primary photochemical product and ***trans*-2Ph** is formed by thermal isomerization (Scheme 3).

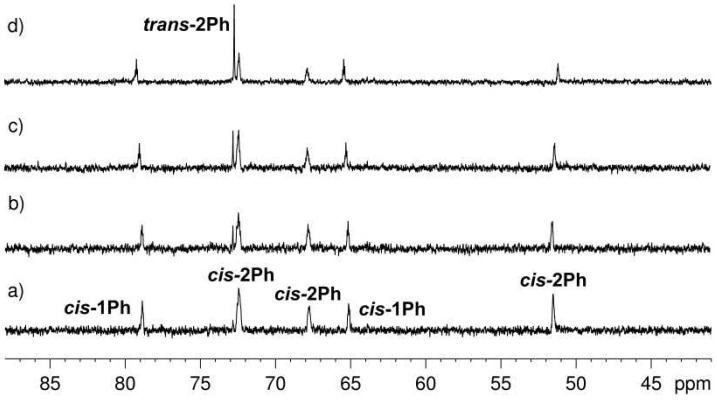

Figure 5. $^{31}P\{^{1}H\}$ NMR spectrum of the products of the photolysis of **1Ph** with GeH_4 at 195 K in tol-d_8. a) Immediately after placing into the NMR spectrometer set at 270 K; b) 5 min after placing into the NMR spectrometer set at 270 K; c) after the NMR spectrometer temperature has been raised from 270 K to 280 K; d) at 295 K. Residual starting material **1Ph** is present in the spectra.

Scheme 3. Photochemical generation of *cis*-2Ph and *cis* 3-Ph followed by thermal conversion to *trans*-2Ph and *trans*-3Ph

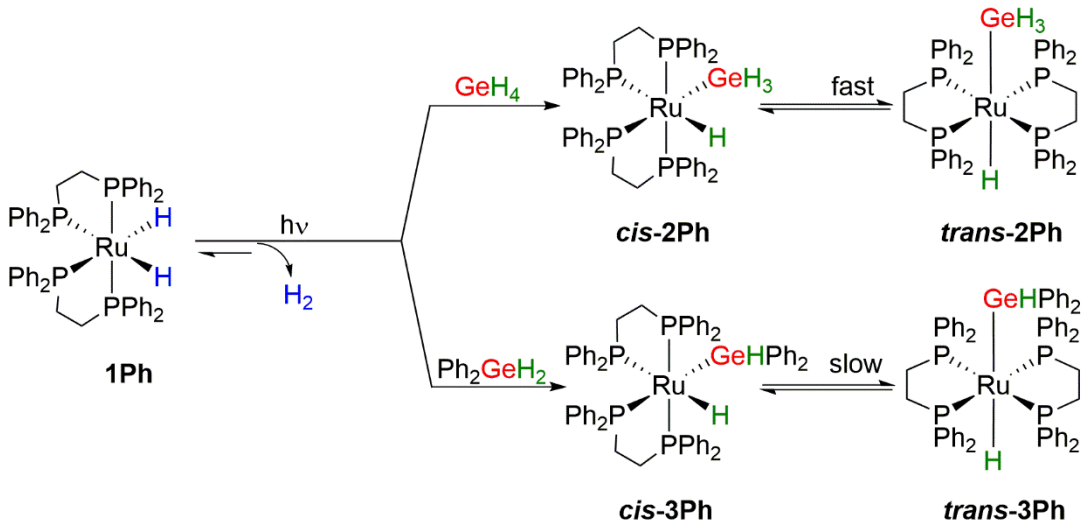

Broadband steady state photolysis of 1Ph with Ph_2GeH_2. In further experiments we examined the reactivity of $Ru(PP)_2(H)_2$ toward diphenylgermane. When comparing the reactivity toward GeH_4 and Ph_2GeH_2, it should be noted that the reactions were carried out with a 5- to 20-fold excess of Ph_2GeH_2 which will have accelerated the thermal reaction, whereas the reactions with GeH_4 were limited by the low solubility of germane. The products could be identified by NMR spectroscopy but isolation was hampered by the difficulty of separating residual diphenylgermane without decomposition of the products. As observed for the reaction with germane gas, **1Ph** does not react thermally at room temperature in the presence of Ph_2GeH_2 in C_6D_6 but does react after 1 day at 70 ºC (30% conversion by NMR) or upon irradiation (λ > 290 nm, 2.5 h, room temperature, 100% NMR conversion) to afford new products. The starting Ph_2GeH_2 shows a singlet at δ 5.20 in C_6D_6 for the GeH protons. After irradiation, the ^{1}H NMR spectrum shows two major hydride-containing products and minor peaks for additional hydride compounds (Figure 6). The hydride representing a *cis*-complex resonates at δ–8.85 ($^2J_{HP(trans)}$ = 69.6, $^2J_{HP(cis)}$ = 19.8 Hz) and the hydride representing a *trans*-species resonates at δ –10.15 (quintet, $^2J_{HP}$ = 20.1 Hz). The ^{1}H NMR spectrum also shows a multiplet at δ 5.08 and a quintet at δ 4.89, belonging to the *cis*- and *trans*-germyl protons respectively. As for ***cis*-2Ph** and ***trans*-2Ph**, the germyl resonances are shifted upfield with respect to the resonances of free substrate. Assignment of these peaks was also

supported by $^{1}H\{^{31}P\}$-^{31}P HMQC spectroscopy. Upon broad-band ^{31}P decoupling, both hydride and germyl resonances simplify to singlets, and give a ratio of 4.5:1, of *cis*- to *trans*-products. The $^{31}P\{^{1}H\}$ NMR spectrum also shows the formation of two new major products: the *cis*-species contains magnetically inequivalent phosphorus atoms, leading to an ABQX spin system. The resonances for the mutually *trans*-phosphorus nuclei, P_A and P_B, present features of an AB quartet, centred at δ 65.3, with coupling constants of $^{2}J_{AB}$ = 237.0, $^{2}J_{AX}$ = 20.0, $^{2}J_{AQ}$ = 15.0, $^{2}J_{BX}$ = 25.0, $^{2}J_{BQ}$ = 9.0 Hz. Each component is split into an apparent doublet of doublet of doublets due to PP coupling. The *trans*-isomer gives a singlet at δ 69.8. On the basis of these results, we assign the two products as *cis*- and *trans*-Ru(dppe)$_2$(GePh$_2$H)H ***cis*-3Ph** and ***trans*-3Ph** respectively (Table 3, Scheme 3). The same products may be obtained at 30% NMR conversion after leaving **1Ph** with Ph_2GeH_2 in C_6D_6 for 1 day at 70 °C, with a *cis:trans* ratio of 4:1.

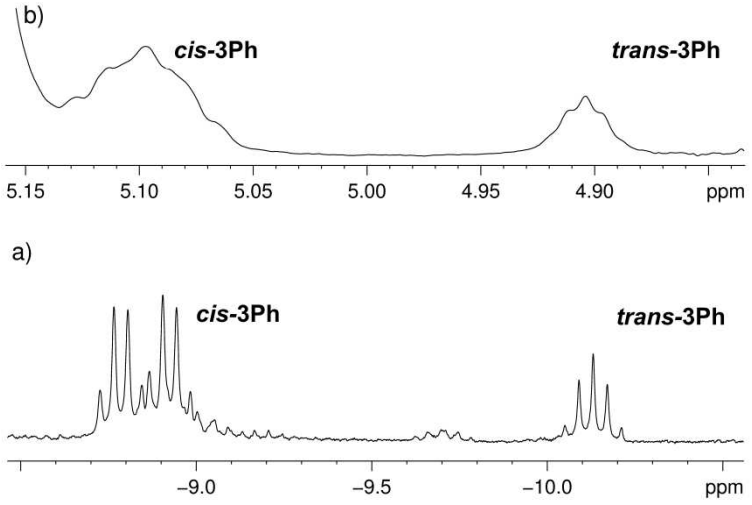

Figure 6. a) Hydride region of the ^{1}H NMR spectrum of the photochemical reaction of **1Ph** with Ph_2GeH_2 in C_6D_6. b) Germyl region of the ^{1}H NMR spectrum of the same reaction.

Change of the phosphine ligand: effects on reaction with diphenylgermane. Ru(dmpe)$_2$H$_2$, **1Me** does react thermally at room temperature in the presence of

diphenylgermane to form the *cis*-product ***cis*-3Me** that exhibits a multiplet in the ^{1}H NMR spectrum at δ–9.58; the reaction was complete upon heating at 70 ^{o}C for 7 hours. Surprisingly, the thermal reaction between **1Me** and diphenylgermane yielded none of the *trans*-product ***trans*-3Me**. The corresponding photochemical reaction of **1Me** with diphenylgermane (λ > 290 nm, 2 h, room temperature, 100% NMR conversion) also yields exclusively the *cis*-product ***cis*-3Me**.

The reactivity of **1Et** with diphenylgermane parallels the behavior of **1Me**. Both thermal (70° C, 7 hours) and photochemical reactions (λ > 290 nm, 2 h, room temperature, 100% NMR conversion) generate selectively the *cis*-product ***cis*-3Et** with its characteristic ^{1}H hydride resonance as a multiplet at δ –10.15.

The complex **1DuPhos** was found to be unreactive both thermally and photochemically towards excess diphenylgermane. The steric bulk both of the complex and the phospholane ligands could account for the inert behavior. NMR data for **3Ph**, **3Me**, and **3Et** are given in Table 3.

***In-situ* monochromatic photolysis of 1Ph with diphenylgermane.** The *in-situ* photochemical reaction of **1Ph** at 355 nm with diphenylgermane at room temperature was shown to produce only *cis*-Ru(dppe)$_2$(GePh$_2$H)H, ***cis*-3Ph** (Figure 7). After leaving the sample overnight, ^{1}H and ^{31}P{^{1}H} NMR spectroscopy showed the presence of ***trans*-3Ph** by resonances at δ –10.15 and 69.8 respectively (See SI). These results show that the photochemical reaction initially forms the *cis*-product ***cis*-3Ph** exclusively, which in turn isomerizes thermally to the *trans*-isomer ***trans*-3Ph**, as already observed for the analogous reaction with GeH_4 (Scheme 3). Comparison of the behavior of GeH_4 and diphenylgermane shows that isomerization of the *cis*-product occurs significantly faster for ***cis*-2Ph** than for ***cis*-3Ph**, perhaps as a result of the smaller steric demand of the germane substituent in comparison to diphenylgermane.

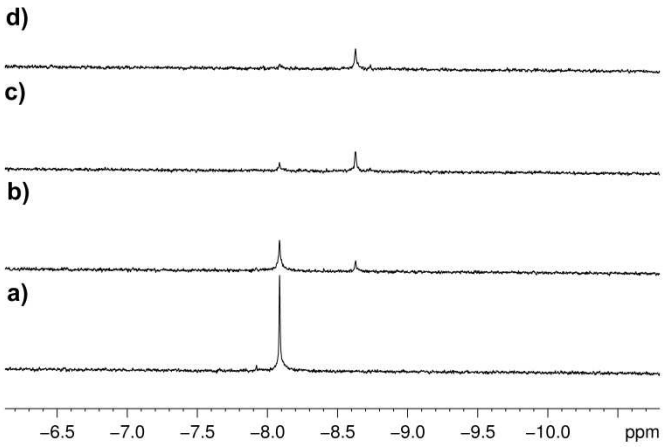

Figure 7. $^{1}H\{^{31}P\}$ NMR spectra of the *in-situ* photolysis of **1Ph** with diphenylgermane after (a) 0, (b) 60, (c) 300, and (d) 420 laser shots. The selective formation of ***cis*-3Ph** is evidenced by the hydride peak at δ –8.85.

Table 3. NMR data for products of photochemical reaction of 1Ph with diphenylgermane in C_6D_6 δ / mult / *J* (Hz)

Product	^{1}H NMR GeH[b]	^{1}H NMR RuH	^{31}P NMR P_{AB}	^{31}P NMR P_X[c]	^{31}P NMR P_Q
***cis*-3Ph**	5.08 (m)	–8.85 (app dq, $^2J_{HP}$ = 70, 20)	65.3 (AB quart of dd, $^2J_{AB}$ = 237, $^2J_{AQ}$ = 20, $^2J_{BX}$ = 25, $^2J_{AX,BQ}$ = 9)	63.4 (m)	45.1 (J_{QA} = 20, J_{QB} = 10)
***cis*-3Me**[a]	5.38 (quin, $^3J_{HP}$ = 4.0)	–9.58 (app dq, $^2J_{HP}$ = 70, 23)	40.9 (AB quart of dd, $^2J_{AB}$ = 244, $^2J_{AX}$ = 21, $^2J_{AQ}$ = 25, $^2J_{BX}$ = 30, $^2J_{BQ}$ = 16)	41.7 (m, $^2J_{XQ}$ = 17)	30.5 (m)
***cis*-3Et**[a]	5.41 (m)	–10.15 (app. dq, $^2J_{HP}$ = 69, 21)	62.5 (AB quart of dd, $^2J_{AB}$ = 235, $^2J_{AX}$ = 21, $^2J_{AQ}$ = 15, $^2J_{BX}$ = 30, $^2J_{BQ}$ = 15)	66.6 (m)	43.8(m)
***trans*-3Ph**	4.89 (quin, $^3J_{HP}$ = 4.0)	–10.15 (quin, $^2J_{HP}$ = 20)	69.8 (s)		

[a] *trans*-isomer not observed
[b] Free $GePh_2H_2$ δ 5.2
[c] P_x lies *trans* to Ge, P_Q lies *trans* to H

Competition reaction: 1Ph + Ph_2SiH_2 + Ph_2GeH_2. Several different types of comparison between the behavior of silanes and germanes towards transition metals were described in the introduction, but no examples of direct competition reactions seem to have been reported. We therefore examined the reaction of **1Ph** with diphenylsilane in C_6D_6 by in-situ laser photolysis and then carried out a reaction with Ph_2SiH_2 and Ph_2GeH_2 in a 1:1 ratio. The reaction with diphenylsilane gave a hydride product, readily assigned as *cis*-[Ru(dppe)($SiPh_2H$)H] by a hydride resonance at δ–8.75 and an SiH resonance at δ5.35 (see SI). Although the hydride resonance of this product overlaps with that of the germyl analogue in the ^{1}H spectrum, clean separation is achieved by ^{31}P decoupling. On carrying out the photochemical reaction with the 1.2:1 mixture of Ph_2SiH_2 + Ph_2GeH_2, the expected two cis products were formed in a ratio of 0.18:1, respectively, showing a clear preference for activation of Ph_2GeH_2 (Figure 8). The same ratio is observed at six different irradiation times during the reaction, indicating that there is no secondary photolysis. There remained the question of whether there is a thermal interconversion between the silyl hydride and the germyl hydride products (eq 1).

$$cis\text{-}[Ru(dppe)_2(SiHPh_2)H] + Ph_2GeH_2 \rightleftharpoons Ru(dppe)_2(GeHPh_2)H + Ph_2SiH_2 \quad (1)$$

When the sample from the competition reaction was heated at 70 °C for 1 h, all the *cis*-[Ru(dppe)$_2$($SiHPh_2$)H] disappeared, while ***cis*-3Ph** remained and ***trans*-3Ph** grew in. A further in-situ photochemical experiment was conducted with **1Ph** and Ph_2SiH_2, giving *cis*-[Ru(dppe)$_2$($SiHPh_2$)H]. Upon warming to 70 °C, the majority of silyl hydride remained, but there was some regeneration of **1Ph**. We then cooled back to room temperature and added Ph_2GeH_2 (equimolar with respect to initial Ph_2SiH_2). No reaction occurred at room temperature, but on heating (1h, 70°C), all *cis*-[Ru(dppe)$_2$($SiHPh_2$)H] was converted to ***cis*-3Ph** and ***trans*-3Ph**. We conclude that the initial product distribution observed in the competition reaction is determined by the photochemical kinetics. However, the reaction in eq 1 strongly favors **3Ph**.

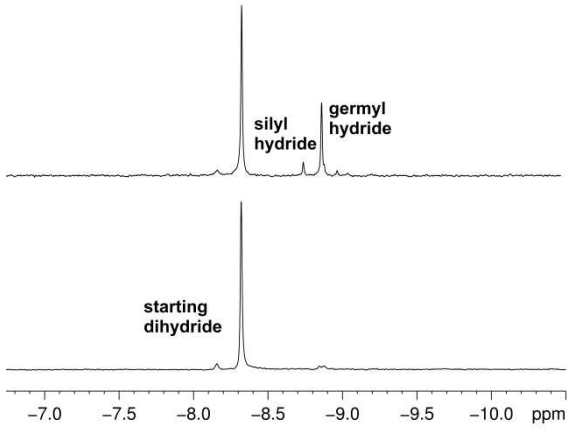

Figure 8. $^{1}H\{^{31}P\}$ NMR spectrum for the competition reaction of **1Ph** with Ph_2SiH_2 + Ph_2GeH_2 (1.2:1). Below, before irradiation; above after laser irradiation at 355 nm for 150 s.

CONCLUSIONS

The Ge–H bond of germane was activated through the photochemical reaction of a series of $Ru(PP)_2H_2$ complexes (PP = dppe, dmpe, depe, DuPhos); the unsaturated intermediate $[Ru(PP)_2]$ formed by photoinduced H_2 reductive elimination proved capable of inserting into the Ge–H bond to form $Ru(PP)_2(GeH_3)H$ species. Both the analysis of the crystal structure of complex ***cis*-2Ph** and the DFT calculations indicated full oxidative addition of the Ge–H bond to the metal center and no residual interaction between the germanium and the hydrogen atoms. The structure of ***cis*-2DuPhos** is less decisive with respect to residual Ge···H(Ru) interaction. The structures calculated by DFT methods are in close agreement with the crystallographic structures. These reactions represent rare examples of oxidative addition of GeH_4 to a metal center and the first to result in crystal structures of metal germyl hydride complexes. Germyl complexes characterized by X-ray or gas phase electron diffraction were prepared by other means.

Diphenylgermane also undergoes Ge–H oxidative addition to $[Ru(PP)]_2$ formed photochemically from $Ru(PP)_2(H)_2$ (PP = dppe, dmpe, depe) as shown by extensive NMR evidence. These precursors also undergo slow thermal oxidative addition, but the

photochemical reactions are much faster. There is no reaction between the very bulky DuPhos complex and Ph_2GeH_2.

The $Ru(PP)_2(GeH_3)H$ and $Ru(PP)_2(GePh_2H)H$ complexes were formed as isomeric *cis* and *trans* products. *In-situ* laser photolysis was used to show that the reaction of $Ru(dppe)_2(H)_2$ with GeH_4 generates the *cis* complex initially, but *cis-trans* isomerization occurs within a few minutes resulting in a 1. 2 c*is :* 1.0 *trans* equilibrium at room temperature. When irradiated at low temperature, the *cis* product is dominant. For the dppe, dmpe and depe species, the equilibrium ratios at room temperature are similar. For DuPhos, we only observe the *cis*-complex, presumably because there is a barrier to isomerization. With $Ru(dppe)_2(GePh_2H)H$, the *cis-trans* ratio is 4.5:1, and equilibration requires hours at room temperature. Only the *cis*-$[Ru(PP)_2(GePh_2H)H]$ complex is observed with depe and dmpe.

The photochemical reactivity of $Ru(PP)_2H_2$ towards GeH_4 and Ph_2GeH_2 is qualitatively similar to the reactions with substituted silanes. Limited data are available for comparisons of the reactivity of the dihydride complexes toward silanes and germanes. The rate constants for the reactions of the transient $[Ru(PP)_2]$ with Et_3SiH have been determined[38] by transient absorption methods. However, with $Ru(DuPhos)_2H_2$, **1DuPhos**, there is no photochemical reaction with Et_3SiH, presumably because of steric hindrance, but this complex is reactive toward Et_2SiH_2 and $PhSiH_3$ with the latter kinetically preferred.[39] In this paper, we demonstrated that a competition reaction between $Ru(dppe)_2(H)_2$ and the two substrates Ph_2SiH_2 and Ph_2GeH_2 results in preferential oxidative addition of the Ge–H bond. This reaction is kinetically controlled (compare reference 52). In addition, we have shown that the thermal reaction of *cis*-$[Ru(dppe)_2(SiHPh_2)H]$ with Ph_2GeH_2 favors formation of *cis*- and *trans*-$[Ru(dppe)_2(GeHPh_2)H]$ implying that the germyl product is more stable thermodynamically than the silyl product.

EXPERIMENTAL SECTION

General Procedures

All operations were performed on a high vacuum line (10^{-5} mbar), under an argon atmosphere on a standard Schlenk (10^{-3} mbar) line, or in a glovebox. Solvents for general use were of AR grade, dried by distillation over sodium and stored under Ar in ampoules fitted with a Young's PTFE stopcock. Hexane was collected from the solvent purification system and dried again by distillation. Deuterated solvents (C_6D_6, C_7D_8) were dried by stirring over potassium and distilled under high vacuum into small ampoules.

$Ru(dppe)_2H_2$ **1Ph**, was synthesized following the reported procedure.[53] Germane gas was prepared according to a procedure based on Woollins.[54] Diphenylgermane was purchased from Fluorochem and transferred into an ampoule in the glove box.

Photochemical reactions at room temperature were performed in pyrex NMR tubes fitted with Young's PTFE stopcocks by using a Philips 125 W medium-pressure mercury vapor lamp with a water filter (5 cm).

NMR spectroscopy was conducted using a Bruker AV500 with a 5 mm BBI probe and a Bruker Advance wide-bore 600 MHz spectrometer with a 5mm BBO probe.

IR spectroscopy was performed using a Unicam Research Series 10000 FTIR instrument.

LIFDI mass spectra were measured on a Waters Micromass GCT Premier orthogonal time-of-flight instrument set to one scan per second with resolution power of 6000 fwhm and equipped with a LIFDI probe from LINDEN GmbH.[55-58] LIFDI m/z values are accurate to 0.01 Da. EI mass spectra were measured on the same instrument under high resolution conditions.

The setup for laser photolysis within an NMR spectrometer is recorded in recent papers.[59] Briefly, laser photolysis was carried out with a pulsed Nd:YAG laser (Continuum Surelite II) fitted with a frequency tripling crystal. Operating conditions were typically 355 nm, 10 Hz repetition rate, laser power 85 mW, energy of a single laser pulse ~ 29.8 mJ. The unfocused laser beam is directed at the base of the spectrometer and reflected up into the probe *via* a mirror. Standard NMR tubes fitted with Young's taps were used. The samples contained 1-2 mg of compound (Abs_{355} ~ 0.7) and approximately 0.4 mL of solvent. NMR spectra were recorded on a Bruker Advance wide-bore 600 MHz spectrometer. Standard NMR

pulse sequences were modified for use with a synchronized laser initiation sequence prior to NMR excitation.

X-ray diffraction data were collected on an Oxford Diffraction SuperNova diffractometer with MoKα radiation (λ = 0.71073 Å) at 110 K unless otherwise noted. Data collection, unit cell determination and frame integration were carried out with the program CrysAlisPro.[60] Absorption corrections were applied using crystal face-indexing and the ABSPACK absorption correction software within CrysAlisPro. Structures were solved and refined using Olex2[61] implementing SHELX algorithms. Structures were solved by either Patterson or direct methods using SHELXS-97 and refined by full-matrix least squares using SHELXL-97.[62] All non-hydrogen atoms were refined anisotropically. Carbon-bound hydrogen atoms were placed at calculated positions with fixed isotropic displacement parameters and refined using a riding model. Hydrides were located by difference map and allowed to refine. Germanium hydrogens were positioned using riding models with the Ge-H distance fixed at 1.53 Å, as use of a difference map either produced an unrealistic model or, for minor components, did not allow identification of a suitable site. Detailed crystallographic data are provided in the ESI.

DFT calculations employing the B3PW91 functional[63] with the version of Grimme's dispersion[64] were performed with the GAUSSIAN 09 series of programs, D01 version.[65] The ruthenium, germanium, and phosphorus atoms were represented by the relativistic effective core potential (RECP) from the Stuttgart group and their associated basis set,[66,67] augmented by polarization functions (α_f = 1.235, Ru; α_d = 0.387, P; α_d = 0.230, Ge).[68,69] The remaining atoms (C, H) were represented by 6-31G(d,p) basis sets.[70] Full optimizations of geometry without any constraint were performed. Calculations of harmonic vibrational frequencies were performed to determine the nature of each extremum. The contributions to the Gibbs free energy were taken at T = 298 K and with P = 1 atm within the harmonic oscillator and rigid rotator approximations.

Analysis of germane and diphenylgermane Ph_2GeH_2. Germane was identified by ^1H and $^{73}Ge\{^1H\}$ NMR spectroscopy and by gas-phase IR spectroscopy. ^1H NMR (C_6D_6) δ 3.05

(s with satellites, $^1J_{HGe}$ = 97.6 Hz) (^{73}Ge 7.73% abundant, I = 9/2). ^{73}Ge NMR spectrum δ – 296.7 (quintet $^1J_{HGe}$ = 97 6 Hz), simplifies to a singlet with proton decoupling.

Diphenylgermane was characterized as follows. ^{1}H NMR (C_6D_6) δ 7.40-7.10 (m, 10 H, C_6H_5), 5.20 (s, 2H, GeH).[8] ^{13}C{^{1}H} NMR δ 135.0 (CGe), 134.0 (C *ortho*), 129.0 (C *para*) and 128.4 (C *meta*) in agreement with the literature.[71] IR (thin film) 2053 cm^{-1} (ν_{GeH}).

Photolysis of 1Ph, 1Me, 1Et, and 1DuPhos with GeH_4. The reaction was performed in an NMR tube fitted with a Young's tap. Approximately 10 mg (ca. 10^{-2} mmol) of complex was added to the tube and dissolved in C_6D_6. To this, germane gas was condensed. The reaction was monitored by ^{1}H and ^{31}P{^{1}H} NMR spectroscopy. After being left overnight to check for a thermal reaction, the sample was irradiated and the progression of the reaction was monitored by ^{1}H and ^{31}P{^{1}H} NMR spectroscopy every 30 min. When the reaction was complete, the sample was analyzed via ^{1}H, ^{13}C{^{1}H} and ^{31}P{^{1}H} NMR spectroscopy as well as LIFDI mass spectrometry. The product complexes ***cis*-2Ph** and ***cis*-2DuPhos** were crystallized by layering with hexane. We generally avoided pumping to dryness and redissolving the resulting solids because of regeneration of initial dihydride precursors.

2Ph. Mass spectrum (LIFDI, *m/z*): 898 (100%, [M – GeH_4]$^+$), 973, 974, 975.00 (8%, [M-H]$^+$), calcd for $C_{52}H_{51}P_4{}^{74}Ge^{102}Ru$ 975.13, difference 0.13 Da, 133 ppm. Mass spectrum (EI, *m/z*) 972.1085 (M-2H_2), calcd for $C_{52}H_{48}{}^{74}GeP_4{}^{102}Ru$ 972.0962, difference 0.0123.

IR (KBr, cm^{-1}): 1927 (medium), 1883 (medium).

***cis*-2Ph.** ^{1}H NMR (500.23 MHz, C_6D_6, 298 K): δ 8.43 (m, br, 2 H), 8.18 (m, br, 2 H), 7.71 (s, br, 2 H), 7.30 (t, 2 H, J_{HH} = 7 Hz), 7.25 (t, 2 H, J_{HH} = 7 Hz), 7.12 (m, 1 H), 7.10 (m, 1 H), 7.00 (m, 10 H), 6.89 (m, 3 H), 6.84 (m, 5 H), 6.70 (pseudo dd, 2 H, J_{HH} = 7 Hz), 6.66 (pseudo dd, 3 H, J_{HH} = 7 Hz), 6.64 (m, 1 H), 6.55 (t, 2 H J_{HH} = 7 Hz), 6.39 (t, 2 H J_{HH} = 7 Hz), 2.94 – 2.80 (m, br, C_2H_4, 2 H), 2.66 (pseudo q, GeH_3, 3 H, J_{PH} = 6 Hz), 2.13 (t, 2 H, C_2H_4, J_{HH} = 3 Hz), 2.01 (m, 4 H), -8.92 (doublet of pseudo quartets, $^2J_{HP}$: J_{AM} = 70 Hz, J_{AX} = 20 Hz, 1 H, Ru-H). ^{31}P{^{1}H} see Table 1. ^{13}C{^{1}H} (125.80, C_6D_6, 298 K): δ 142.00 (pseudo d, Ph quaternary, J_{CP} = 10 Hz), 141.86 (pseudo d, Ph quaternary, J_{CP} = 11 Hz), 138.55 (m, Ph q quaternary),

137.86 (m, Ph), 137.51 (s, Ph), 137.31 (s, Ph), 134.65 (m, Ph), 133.64 (s, Ph), 133.15 (m, Ph), 132.15 (d, Ph, J_{CP} = 10 Hz), 131.92 (d, Ph, J_{CP} = 12 Hz), 131.83 (d, Ph, J_{CP} = 10 Hz), 130.87 (m, Ph), 129.15 (s, Ph), 128.62 (s, Ph), 127.68 (s, Ph), 127.40 (m, Ph), 32.62 (br, C_2H_4), 27.22 (br, C_2H_4).

IR of ***cis*-2Ph** calculated by DFT (corrected with a factor of 0.96, cm^{-1}): 1926 ν_{RuH} (intense), ν_{GeH} (intense) 1903, 1852, 1819.

***trans*-2Ph**. ^1H NMR (500.23 MHz, C_6D_6, 298 K): δ 7.79 (s, br, 6 H), 7.66 (m, br, 3 H), 6.99 (m, 16 H), 6.94 (pseudo dd, 15 H), 2.56 (m, 3 H, C_2H_4), 2.50 (pseudo q, GeH_3, 3 H, J_{PH} = 3 Hz), 1.78 (m, 2 H, C_2H_4), -8.48 (quin, 0.7 H, Ru-H, $^2J_{PH}$ = 19 Hz). $^{31}P\{^1H\}$ (202.51 MHz, C_6D_6, 298 K): δ 72.20 (s). $^{13}C\{^1H\}$ (125.80, C_6D_6, 298 K): δ 141.22 (m, Ph quaternary), 134.08 (m, Ph), 132.84 (s, Ph), 128.6-127.4 (Ph), 34.27 (pseudo d, C_2H_4, J_{CP} = 12 Hz), 34.05 (pseudo d, C_2H_4, J_{CP} = 15 Hz).

IR calculated by DFT (corrected with a factor of 0.96, cm^{-1}): 1959 ν_{RuH} (medium), 1824 ν_{GeHsym} (intense), 1818 & 1792 $\nu_{GeH\ antisym}$ (intense).

2Me. Mass spectrum (LIFDI, *m/z*) 480.02 (M^+, 100%) Calcd for $C_{12}H_{36}{}^{74}GeP_4{}^{102}Ru$ 480.002, difference 0.018

***cis*-2Me.** ^1H NMR (500.23 MHz, 298 K, C_6D_6): δ 3.11 (m, 1 H, GeH_3, $^3J_{HP}$ = 7 Hz), 1.60 to 0.87 (CH_2CH_2 and CH_3), -10.09 (doublet of pseudo quartets, $^2J_{HP}$: J_{AM} = 72 Hz, J_{AX} = 23 Hz, 1 H, Ru-H). $^{31}P\{^1H\}$ see Table 1. It was not possible to distinguish the aliphatic protons of the *cis*-isomer from those of the *trans*-isomer. Most resonances in the aliphatic region are doublets that simplify to singlets when ^{31}P decoupled ($J_{PH} \simeq 6$ Hz).

***trans*-2Me.** ^1H NMR (500.23 MHz, 298 K, C_6D_6): δ 2.71 (quin, 3 H, GeH_3, $^3J_{PH}$ = 4 Hz), 1.49 to 1.19 (CH_2CH_2 and CH_3) -11.20 (quin, 1 H, Ru-H $^2J_{HP}$ = 21 Hz). $^{31}P\{^1H\}$ see Table 1.

2Et. Mass spectrum (LIFDI, *m/z*) 514 (60%, $[M - GeH_4]^+$), 592.06 (100%, $[M]^+$), calcd for $C_{20}H_{52}P_4{}^{74}Ge{}^{102}Ru$ 592.13, difference 68 mDa.

IR (KBr, cm^{-1}): 1838 (intense), 1876 (shoulder).

***cis*-2Et.** ^{1}H NMR (500.23 MHz, 298 K, C_6D_6): δ 2.90 (quin, 1 H, GeH_3, $^{3}J_{HP}$ = 6 Hz), 2.33 (dquart, 4 H, CH_2CH_3, J_{HH} = 15, J_{HH} = 7 Hz), 1.72 (dquart, 3.8 H, CH_2CH_3, J_{HH} = 14, J_{HH} = 7 Hz), 1.63 (br m, 4 H, CH_2CH_3), 1.43 (br m, 4 H, CH_2CH_2), 1.24 (br m, 4 H, CH_2CH_2), 1.11 (dquart, 4 H, CH_2CH_3, J_{HH} = 14, J_{HH} = 7 Hz), 0.97 (pseudo t, 24 H, CH_2CH_3, J_{HH} = 7 Hz), -10.74 (doublet of pseudo quartets, $^{2}J_{HP}$: J_{AM} = 71, J_{AX} = 22, 0.4 Hz 1H, Ru-H). ^{31}P{^{1}H} see Table 1. ^{13}C {^{1}H} NMR (125.78 MHz, 298 K, C_6D_6): δ 24.73 (t, CH_2CH_3, J_{PC} = 7 Hz), 23.98 (t, CH_2CH_3, J_{PC} = 6 Hz), 23.90 (m, CH_2CH_2), 9.32 (s, CH_2CH_3), 8.84 (s, CH_2CH_3). It was not possible to distinguish the aliphatic protons and carbons of the minor *cis*-isomer from those of the *trans*-isomer.

***trans*-2Et.** ^{1}H NMR (500.23 MHz, 298 K, C_6D_6): δ 2.88 (quin, 3 H, GeH_3, $^{3}J_{PH}$ = 4 Hz), -11.29 (quin, 1 H, Ru-H $^{2}J_{HP}$ = 20 Hz). ^{31}P {^{1}H} NMR (161.99 MHz, 298 K, C_6D_6): δ 66.27 (s). ^{13}C {^{1}H} NMR (125.78 MHz, 298 K, C_6D_6): δ 24.73 (t, CH_2CH_3, J_{PC} = 7), 23.98 (t, CH_2CH_3, J_{PC} = 6), 23.90 (m, CH_2CH_2), 9.32 (s, CH_2CH_3), 8.84 (s, CH_2CH_3).

Cis-2DuPhos. Mass spectrum (LIFDI, *m/z*): 714 (62 %, $[M - GeH_2]^+$), 792.19 (100 %, M^+), calcd for $C_{36}H_{60}P_4{}^{74}Ge^{102}Ru$ 792.19.

IR (KBr, cm^{-1}): 1910 (intense) ν_{RuH}, 1867 (medium) DFT (calculated corrected with a factor of 0.96, cm^{-1}): 1949 ν_{RuH} (medium), 1832 ν_{GeHsym} (intense), 1818, 1808 $\nu_{GeH\ antisym}$ (intense).

^{1}H NMR (500.23 MHz, C_6D_6, 298 K): δ 7.64 - 6.90 (8 H, Ph), 3.75 (pseudoquintet, J_{PH} = 5 Hz, 3 H, GeH_3), 3.27 (m, 1 H, CH), 2.90 (m, 1 H, CH), 2.57(m, 1 H, CH), 2.53 (m, 1 H, CH), 2.48 (m, 2 H, CH_2), 2.36 (m, 1 H, CH_2), 2.17 (m, 1 H, CH), 2.00 (m, 1 H, CH), 1.98 – 1.80 (m, 5 H, CH_2), 1.78 (m, 1 H, CH), 1.74 (m, 1 H, CH_2), 1.72 (dd, J_{PH} = 16, J_{HH} = 7 Hz, 3 H, CH_3), 1.68 (dd, J_{PH} = 18, J_{HH} = 8 Hz, 3 H, CH_3), 1.64 (m, 1 H, CH_2), 1.60 (m, 1 H, CH), 1.58 (m, 1 H, CH_2), 1.51 (dd, J_{PH} = 18, J_{HH} = 8 Hz, 3 H, CH_3), 1.41(m, 1 H, CH_2), 1.37 (dd, J_{PH} = 16, J_{HH} = 7 Hz, 3 H, CH_3), 1.28 (m, 2 H, CH_2), 1.24 (m, 1 H, CH_2), 0.60 (m, 1 H, CH_2), 0.30 - 0.20 (m, 12 H, CH_3), -9.36 (ddt multiplet, $^{2}J_{HP}$: J_{AM} = 68, J_{AQ} = 24, J_{AX} = 17 Hz, 1 H, Ru-H). ^{31}P NMR see Table 1. ^{13}C {^{1}H} (125.80, C_6D_6, 298 K): δ 130.14 – 126.37 (Ph), 52.33 (m, C(**H**)CH_3) , 46.33

(m, C(**H**)CH_3), 43.67 (m, 2 C(**H**)CH_3), 42.80 (m, CH_2), 39.30 (m, C(**H**)CH_3), 38.49 (m, C(**H**)CH_3), 38.08 (m, C(**H**)CH_3), 38.02 (m, CH_2), 37.53 (s, CH_3), 37.20 (s, CH_3), 36.93 (m, CH_2), 35.51 (s, CH_3), 35.09 (s, CH_2), 34.73 (s, CH_2), 34.40 (s, CH_2), 33.24 (m, C(**H**)CH_3), 22.55 (m, CH_3), 22.35 (m, CH_3), 19.68 (m, CH_3), 19.43 (s, CH_3), 19.34 (s, CH_3), 18.61 (m, CH_3), 13.70 (m, CH_3), 13.46 (m, CH_3).

Photolysis of 1Ph, 1Me, 1Et and 1DuPhos with diphenylgermane. Approximately 10 mg (ca. 10^{-2} mmol) of complex and $GePh_2H_2$ (10 µl, $5.3x10^{-2}$ mmol) were added to an NMR tube fitted with a Young's tap the tube and dissolved in C_6H_6. After leaving overnight to check for a thermal reaction, the sample was irradiated and the progress of the reaction was monitored by ^1H and $^{31}P\{^1H\}$ NMR spectroscopy every 30 min (for example, the reaction of **1Et** with Ph_2GeH_2 was complete in 2 h). When the reaction was complete, the C_6H_6 solvent was removed *in vacuo* and the solid was dissolved in C_6D_6. The sample was analysed *via* ^1H, $^{13}C\{^1H\}$ and $^{31}P\{^1H\}$ NMR spectroscopy and LIFDI mass spectrometry. The samples could not be pumped to dryness because Ph2GeH2 is not sufficiently volatile.

3-Ph. Mass spectrum (LIFDI, *m/z*): 1126.29 (20%, $[M-H_2]^+$) Calcd for $C_{64}H_{58}{}^{74}GeP_4{}^{102}Ru$ 1126.18, difference 0.11, 898.16 (100%, $[M-GeH_2Ph_2]^+$).

***cis*-3Ph.** ^1H NMR (500.23 MHz, C_6D_6, 298 K): δ 8.09, 7.77, 7,43, 7.23, 7.20, 7.19, 7.04, 6.40 (m, br, *o, m, p*-phenyl resonances), , 2.84-1.83 (m, br, C_2H_4, 2H), 5.08 (pseudo q, GeH, 2 H, J_{PH} = 7 Hz), -8.85 (doublet of pseudo quartets, $^2J_{HP}$: J_{AM} = 70 Hz, J_{AX} = 20 Hz, 1 H, Ru-H). $^{31}P\{^1H\}$ see Table 3. $^{13}C\{^1H\}$ (125.80, C_6D_6, 298 K): δ 138.3 to 125.6 (m, phenyl resonances), 33.8 to 29.2 (m, alkyl resonances).

***trans*-3Ph**. ^1H NMR (500.23 MHz, 298 K, C_6D_6): δ 7.60 (m, *o, p*-phenyl resonances, 24H), 6.92 (m, *m*-phenyl resonances, 16H), 4.89 (quin, 3 H, GeH, $^3J_{PH}$ = 4 Hz), 2.72 (m, CH_2CH_2, 4H), 2.08 (m, CH_2CH_2, 4H) -10.15 (quin, 1 H, Ru-H $^2J_{HP}$ = 20 Hz). $^{31}P\{^1H\}$ NMR see Table 3. $^{13}C\{^1H\}$ (125.80, C_6D_6, 298 K): δ 138.3 to 125.6 (m, phenyl resonances), 32.8 (m, alkyl resonances).

3-Me. Mass spectrum (LIFDI, *m/z*): 632.08 (100%, M^+), calcd for $C_{24}H_{44}{}^{74}GeP_4{}^{102}Ru$

632.06, difference 0.02.

***cis*-3Me.** ^{1}H NMR (500.23 MHz, 298 K, C_6D_6): δ 5.38 (quin, 2 H, GeH, $^{3}J_{HP}$ = 4 Hz), 1.78 to 1.12 (CH_2CH_2 and CH_3), -9.58 (doublet of pseudo quartets, $^{2}J_{HP}$: J_{AM} = 70 Hz, J_{AX} = 23 Hz, 1 H, Ru-H). $^{31}P\{^{1}H\}$ see Table 3. $^{13}C\{^{1}H\}$ (125.80, C_6D_6, 298 K): δ 138.2 to 134.5 (m, phenyl resonances), 34.5 to 19.3 (m, alkyl resonances).

3-Et. Mass spectrum (LIFDI, *m/z*): 744.21 (35%, $[M\text{-}H_2]^+$), 668 (20%), 514 (50%), 456 (100%) Calcd for $C_{32}H_{60}{}^{74}GeP_4{}^{102}Ru$ 744.19, difference 0.02

***cis*-3Et.** ^{1}H NMR (500.23 MHz, 298 K, C_6D_6): δ 5.41 (m, 2 H, GeH, $^{3}J_{HP}$ = 4 Hz), 1.62 to 0.72 (CH_2CH_2 and CH_2CH_3), -10.15 (doublet of pseudo quartets, $^{2}J_{HP}$: J_{AM} = 69 Hz, J_{AX} = 21 Hz, 1 H, Ru-H). $^{31}P\{^{1}H\}$ see Table 3. $^{13}C\{^{1}H\}$ (125.80, C_6D_6, 298 K): δ 138.3 to 134.8 (m, phenyl resonances), 28.3 to 19.4 (m, alkyl resonances).

***In-situ* photolysis of 1Ph with diphenylgermane.** A sample of **1Ph** in C_6D_6 was made up in an NMR tube fitted with a Young's tap. The concentration was set to give an absorbance of ca. 0.7 at λ = 355 nm by UV-vis spectroscopy. To this solution, diphenylgermane was added to give a ratio of diphenylgermane:complex of 20:1. The tube was exposed to the laser in sets of 30 shots, and checked by $^{1}H\{^{31}P\}$ and $^{31}P\{^{1}H\}$ NMR spectroscopy following each set. The reaction was stopped after 900 laser shots and checked by ^{1}H, $^{1}H\{^{31}P\}$ and $^{31}P\{^{1}H\}$ NMR spectroscopy.

***In-situ* laser photolysis of Ru(dppe)$_2$H$_2$ with germane.** A sample of **1Ph** in C_6D_6 was made up as above. To this, germane gas was condensed. The reaction was exposed to the laser in sets of 15 shots and checked by $^{1}H\{^{31}P\}$ and $^{31}P\{^{1}H\}$ NMR spectroscopy following each set. The reaction was stopped after 315 laser shots and checked by ^{1}H, 1H$\{^{31}P\}$ and $^{31}P\{^{1}H\}$ NMR spectroscopy.

Low temperature photolysis of 1Ph with germane. A sample of **1Ph** (6 mg) in protio-toluene was made up in an NMR tube and germane gas was condensed. The reaction was photolyzed for 3 h at 195 K in an unsilvered glass Dewar flask filled with acetone and dry ice. The sample was transferred to the NMR spectrometer, set at a temperature of 270 K, and

analyzed *via* $^{31}P\{^{1}H\}$ NMR spectroscopy. The temperature was raised to 280 K and then 295 K, and the sample analyzed at each temperature by $^{31}P\{^{1}H\}$ NMR spectroscopy.

Competition reaction with Ph_2SiH_2 and Ph_2GeH_2. A solution of **1Ph** in C_6D_6 was made up as above. To this, equimolar quantities of Ph_2SiH_2 and Ph_2GeH_2 were added and the exact ratio determined by ^{1}H NMR to be Si:Ge = 1.2:1. $^{1}H\{^{31}P\}$ and $^{31}P\{^{1}H\}$ NMR spectra were acquired at time 0 and after 30, 90, 150 and 270 s of in-situ laser photolysis.

SAFETY WARNING

The synthesis of germane (see Supporting information) generates significant quantities of hydrogen. Precautions should be taken to avoid any pressure build-up.

ASSOCIATED CONTENT

Supporting information

The Supporting Information is available free of charge on the ACS Publications website at DOI:. Details of synthesis and spectra of germane, NMR and mass spectra of products, crystallographic data and molecular structures of minor components of crystals. Experimental datasets associated with this paper were deposited with the University of York library.

AUTHOR INFORMATION

Corresponding Authors

*E-mail for R.N.P: robin.perutz@york.ac.uk

*E-mail for B.P.: barbara.procacci@york.ac.uk

ORCID

Mary Grellier: 0000-0002-1823-3086

Barbara Procacci: 0000-0001-7044-0560

Robin N. Perutz: 0000-0001-6286-0282

Sylviane Sabo-Etienne: 0000-0001-7264-556X

Notes

The authors declare no competing financial interest

ACKNOWLEDGEMENTS

We are grateful to EPSRC and CNRS for funding and Dr Naser Jasim and Dr Pedro Aguiar for experimental assistance. KAS thanks the French Ministry of Research for a PhD fellowship. We were also granted access for this research to the HPC resources of the CALMIP supercomputing center under the allocation 2018-[p0909], Toulouse, France.

REFERENCES

(1) Corey, J. Y.; Braddock-Wilking, J. Reactions of hydrosilanes with transition-metal complexes: Formation of stable transition-metal silyl compounds. *Chem. Rev.* **1999,** *99*, 175-292.

(2) Corey, J. Y. Reactions of hydrosilanes with transition metal complexes and characterization of the products. *Chem. Rev.* **2011,** *111*, 863-1071.

(3) Corey, J. Y. Reactions of hydrosilanes with transition metal complexes. *Chem. Rev.* **2016,** *116*, 11291-11435.

(4) Smart, K. A.; Mothes-Martin, E.; Vendier, L.; Perutz, R. N.; Grellier, M.; Sabo-Etienne, S. A ruthenium dihydrogen germylene complex and the catalytic synthesis of digermoxane. *Organometallics* **2015,** *34*, 4158-4163.

(5) Luo, Y. *Comprehensive handbook of chemical bond energies*; CRC Press: Boca Raton, FL, 2007.

(6) Pullen, B. P.; Carlson, T. A.; Moddeman, W. E.; Schweitzer, G. K.; Bull, W. E.; Grimm, F. A. Photoelectron spectra of methane, silane, germane, methyl fluoride, difluoromethane, and trifluoromethane. *J. Chem. Phys.* **1970,** *53*, 768-782.

(7) Nakamoto, K. *Infrared and Raman spectra of inorganic and coordination compounds*; 3rd Ed ed.; Wiley: New York, 1978.

(8) (a) Clark, K. B.; Griller, D. The Ge-H bond-dissociation energies of organogermanes - a laser-induced photoacoustic study. *Organometallics* **1991,** *10*, 746-750. (b) Becerra, R.; Walsh, R.

Thermochemistry of germanium and organogermanium compounds. *Phys. Chem. Chem. Phys.* DOI: 10.1039/c8cp06208k.

(9) Cotton, F. A.; Wilkinson, G.; Murillo, C. A.; Bochmann, M. *Advanced inorganic chemistry*; 6th edition ed.; Wiley: New York, 1999.

(10) Ebsworth, E. A. V.; Fraser, T. E. Reactions of silanes and germanes with iridium complexes .2. Adducts of silyl and germyl halides and related molecules with trans-carbonylhalogenobis(triethylphosphine)Iridium(I). *J. Chem. Soc., Dalton Trans.* **1979**, 1960-1964.

(11) Zuzek, A. A.; Parkin, G. Oxidative addition of SiH_4 and GeH_4 to $Ir(PPh_3)_2(CO)Cl$: structural and spectroscopic evidence for the formation of products derived from cis oxidative addition. *Dalton Trans.* **2015,** *44*, 2801-2808.

(12) Luo, X. L.; Kubas, G. J.; Burns, C. J.; Bryan, J. C.; Unkefer, C. J. The first transition-metal η^2-SiH_4 complexes, cis-$Mo(\eta^2\text{-}SiH_4)(CO)(R_2PC_2H_4PR_2)_2$, and unprecedented tautomeric equilibrium between an η^2-silane complex and a hydridosilyl species - a model for methane coordination and activation. *J. Am. Chem. Soc.* **1995,** *117*, 1159-1160.

(13) Vincent, J. L.; Luo, S.; Scott, B. L.; Butcher, R.; Unkefer, C. J.; Burns, C. J.; Kubas, G. J.; Lledós, A.; Maseras, F.; Tomàs, J. Experimental and theoretical studies of bonding and oxidative addition of germanes and silanes, $EH_{4-n}Ph_n$ (E = Si, Ge; n=0-3), to $Mo(CO)(diphosphine)_2$. The first structurally characterized germane sigma complex. *Organometallics* **2003,** *22*, 5307-5323.

(14) Ben Said, R.; Hussein, K.; Tangour, B.; Sabo-Etienne, S.; Barthelat, J. C. A DFT study of germane activation in ruthenium complexes. Sigma-coordination versus oxidative addition. *New J. Chem.* **2003,** *27*, 1385-1391.

(15) Braddock-Wilking, J.; Corey, J. Y.; White, C.; Xu, H. A.; Rath, N. P. Reaction of diphenylgermane with $(Ph_3P)_2Pt(\eta^2\text{-}C_2H_4)$: Generation of mono- and dinuclear complexes containing Pt-Ge

bonds. X-ray crystal structure determination of $[(Ph_3P)Pt(\mu\text{-}\eta^2\text{-}H\text{-}GePh_2)]_2$. *Organometallics* **2005,** *24*, 4113-4115.

(16) Tanabe, M.; Ishikawa, N.; Osakada, K. Preparation and structure of a new dipalladium complex with bridging diphenylgermyl ligands. Diverse reactivities of $Pd(PCy_3)_2$ and $Pt(PCy_3)_2$ toward Ph_2GeH_2. *Organometallics* **2006,** *25*, 796-798.

(17) Ahrens, T.; Ahrens, M.; Braun, T.; Braun, B.; Herrmann, R. Synthesis of a rhodium(I) germyl complex: a useful tool for C-H and C-F bond activation reactions. *Dalton Trans.* **2016,** *45*, 4716-4728.

(18) Tanabe, M.; Tanaka, K.; Omine, S.; Osakada, K. A triangular triplatinum(0) complex with bridging germylene ligands: insertion of alkynes into the Pt-Ge bond rather than the Pt-Pt bond. *Chem. Commun.* **2014,** *50*, 6839-6842.

(19) Mobarok, M. H.; McDonald, R.; Ferguson, M. J.; Cowie, M. Germyl- and germylene-bridged complexes of Rh/Ir and subsequent chemistry of a bridging germylene group. *Inorg. Chem.* **2012,** *51*, 4020-4034.

(20) Carré, F.; Colomer, E.; Corriu, R. J. P.; Vioux, A. Stereochemistry of the Insertion of Manganese into Si-H and Ge-H Bonds - Complexes Containing a 2-Electron, 3-Center Mn...H...Si (or Ge) Interaction. *Organometallics* **1984,** *3*, 1272-1278.

(21) Lichtenberger, D. L.; Raichaudhuri, A. Electronic-structure factors of Ge-H bond activation by transition-metals - Photoelectron-spectra of $[Mn(\eta^5\text{-}C_5H_5)(CO)_2(HGePh_3)]$, $[Mn(\eta^5\text{-}C_5H_4Me)(CO)_2(HGePh_3)]$, and $[Mn(\eta^5\text{-}C_5Me_5)(CO)_2(HGePh_3)]$. *J. Chem. Soc., Dalton Trans.* **1990**, 2161-2166.

(22) Sabo-Etienne, S.; Hernandez, M.; Chung, G.; Chaudret, B. Substitution-reactions of coordinated dihydrogen by weakly coordinating ligands - Preparation of $RuH_2(N_2)_2(PCy_3)_2$ and $RuH_2(\eta^2\text{-}H_2)(HEPh_3)(PCy_3)_2$ (E=Si, Ge). *New J. Chem.* **1994,** *18*, 175-177.

(23) Hussein, K.; Marsden, C. J.; Barthelat, J. C.; Rodriguez, V.; Conejero, S.; Sabo-Etienne, S.; Donnadieu, B.; Chaudret, B. X-ray structure and theoretical studies of $RuH_2(\eta^2\text{-}H_2)(\eta^2\text{-}H\text{-}$

SiPh)$(PCy)_2$, a complex with two different η^2-coordinated sigma bonds. *Chem. Commun.* **1999**, 1315-1316.

(24) Shinohara, A.; Mcbee, J.; Tilley, T. D. Germylene and silylene complexes of molybdenum via E-H (E = Ge, Si) bond activations: Steric influences on intramolecular MoH...E interactions. *Inorg. Chem.* **2009,** *48*, 8081-8083.

(25) Fasulo, M. E.; Tilley, T. D. Synthesis and reactivity of cationic ruthenium germylene complexes $[Cp^*(PiPr_3)RuH_2(=GeRR')]^+$. *Chem. Commun.* **2012,** *48*, 7690-7692.

(26) Mork, B. V.; Tilley, T. D.; Schultz, A. J.; Cowan, J. A. Silylene hydride complexes of molybdenum with silicon-hydrogen interactions: Neutron structure of η^5-$C_5Me_5)(Me_2PCH_2CH_2PMe_2)Mo(H)(SiEt_2)$. *J. Am. Chem. Soc.* **2004,** *126*, 10428-10440.

(27) Takaoka, A.; Mendiratta, A.; Peters, J. C. E-H bond activation reactions (E = H, C, Si, Ge) at ruthenium: terminal phosphides, silylenes, and germylenes. *Organometallics* **2009,** *28*, 3744-3753.

(28) Atheaux, I.; Donnadieu, B.; Rodriguez, V.; Sabo-Etienne, S.; Chaudret, B.; Hussein, K.; Barthelat, J. C. A unique coordination of SiH_4: Isolation, characterization, and theoretical study of $(PR_3)_2H_2Ru(SiH_4)RuH_2(PR_3)_2$. *J. Am. Chem. Soc.* **2000,** *122*, 5664-5665.

(29) Ben Said, R.; Hussein, K.; Barthelat, J. C.; Atheaux, I.; Sabo-Etienne, S.; Grellier, M.; Donnadieu, B.; Chaudret, B. Redistribution at silicon by ruthenium complexes. Bonding mode of the bridging silanes in $Ru_2H_4(\mu\text{-}\eta^2\text{:}\eta^2\text{:}\eta^2\text{-}SiH_4)(PCy_3)_4$ and $Ru_2H_2(\mu\text{-}\eta^2\text{:}\eta^2\text{-}H_2Si(OMe)_2)_3(PCy_3)_2$. *Dalton Trans.* **2003**, 4139-4146.

(30) Comanescu, C. C.; Iluc, V. M. E-H (E = B, Si, Ge) bond activation of pinacolborane, silanes, and germanes by nucleophilic palladium carbene complexes. *Chem. Commun.* **2016,** *52*, 9048-9051.

(31) Tanabe, M.; Omine, S.; Ishikawa, N.; Osakada, K.; Hayashi, Y.; Kawauchi, S. Bond formation and coupling between germyl and bridging germylene ligands in dinuclear palladium(I) complexes. *Angew. Chem., Int. Ed.* **2015,** *54*, 2679-2683.

(32) Zyder, M.; Kochel, A.; Handzlik, J.; Szymanska-Buzar, T. Photochemical reaction of $Mo(CO)_6$ with Et_2GeH_2: NMR and DFT sudies of reaction products; crystal structure of a novel complex [{Mo(μ -η^2-H-$GeEt_2$)$(CO)_4$}$_2$]. *Organometallics* **2009,** *28*, 5857-5865.

(33) Zyder, M.; Szymanska-Buzar, T. Activation of the Ge-H bond of Et_3GeH in photochemical reaction with molybdenum(0) carbonyl complexes and hydrogermylation of norbornadiene. *J. Organomet. Chem.* **2009,** *694*, 2110-2113.

(34) Handzlik, J.; Szymanska-Buzar, T. The formation of a sigma-bond complex vs. an oxidation addition product in reaction of [$M(CO)_4$(η^4-nbd)] (M = W, Mo) and H-EEt_3 (E = Si, Ge, Sn): DFT optimized structures and predicted chemical shifts of hydride ligands. *J. Organomet. Chem.* **2014,** *769*, 136-143.

(35) Handzlik, J.; Kochel, A.; Szymanska-Buzar, T. H-Ge bond activation by tungsten carbonyls: An experimental and theoretical study. *Polyhedron* **2012,** *31*, 622-631.

(36) Zhang, N.; Sherbo, R. S.; Bindra, G. S.; Zhu, D.; Budzelaar, P. H. M. Rh and Ir beta-diiminate complexes of boranes, silanes, germanes, and stannanes. *Organometallics* **2017,** *36*, 4123-4135.

(37) Hall, C.; Jones, W. D.; Mawby, R. J.; Osman, R.; Perutz, R. N.; Whittlesey, M. K. Matrix-Isolation and transient photochemistry of $Ru(Dmpe)_2H_2$ - Characterization and Reactivity of $Ru(Dmpe)_2$ (Dmpe = $Me_2PCH_2CH_2PMe_2$). *J. Am. Chem. Soc.* **1992,** *114*, 7425-7435.

(38) Cronin, L.; Nicasio, M. C.; Perutz, R. N.; Peters, R. G.; Roddick, D. M.; Whittlesey, M. K. Laser flash photolysis and matrix isolation studies of $Ru[R_2PCH_2CH_2PR_2]_2H_2$. (R = C_2H_5, C_6H_5, C_2F_5): control of oxidative addition rates by phosphine substituents. *J. Am. Chem. Soc.* **1995,** *117*, 10047-10054.

(39) Câmpian, M. V.; Perutz, R. N.; Procacci, B.; Thatcher, R. J.; Torres, O.; Whitwood, A. C. Selective photochemistry at stereogenic metal and ligand centers of cis-[Ru(diphosphine)$_2$$(H)_2$]: preparative, NMR, solid state and laser flash studies. *J. Am. Chem. Soc.* **2012,** *134*, 3480-3497.

(40) Torres, O.; Procacci, B.; Halse, M. E.; Adams, R. W.; Blazina, D.; Duckett, S. B.; Eguillor, B.; Green, R. A.; Perutz, R. N.; Williamson, D. C. Photochemical pump and NMR probe: chemically created NMR coherence on a microsecond time scale. *J. Am. Chem. Soc.* **2014,** *136*, 10124-10131.

(41) Lindeman, L. P.; Wilson, M. K. Rotational Constants of GeH_3D and $GeHD_3$. *J. Chem. Phys.* **1954,** *22*, 1723-1727.

(42) Beagley, B.; Monaghan, J. J. Electron diffraction study of digermane. *Trans. Faraday Soc.* **1970,** *66*, 2745-2748.

(43) Alvarez, S. A cartography of the van der Waals territories. *Dalton Trans.* **2013,** *42*, 8617-8636.

(44) Albertin, G.; Antoniutti, S.; Castro, J.; Scapinello, F. Preparation and reactivity of germyl complexes of ruthenium and osmium stabilised by cyclopentadienyl, indenyl and tris(pyrazolyl)borate fragments. *J. Organomet. Chem.* **2014,** *751*, 412-419.

(45) Gäde, W. E.; Weiss, E. Carbonyl(cyclopentadienyl)mangan Verbindungen mit Mn-GeH_3 und Mn-$GeCl_3$ Gruppen. Die Krystallstrukturen von $[(CH_3)_4N][\eta\text{-}CH_3C_5H_4Mn(CO)_2(GeH_3]$ und $\eta\text{-}CH_3C_5H_4Mn(CO)_2(GeCl_3)_2$. *Chem. Ber.* **1981,** *114*, 2399-2404.

(46) Albertin, G.; Antoniutti, S.; Castro, J. Synthesis and reactivity of germyl complexes of manganese and rhenium. *J. Organomet. Chem.* **2012,** *696*, 4191-4201.

(47) Pohlmann, H.; Weiss, E. GeH_3-Substituted carbonyl metallates and carbonyl(cyclopentadienyl) metallates with V, Nb, Cr, Mo, W, Re, CO, and Ni - preparative and X-ray-investigations. *Chem. Ber.-Rec.* **1988,** *121*, 1427-1433.

(48) Melzer, D.; Weiss, E. GeH_3-substituted carbonylmetallates of Cr, W, Mn and CO - the crystal-structure of $[PPh_4][Cr(CO)_5GeH_3]$. *Chem. Ber.-Rec.* **1984,** *117*, 2464-2468.

(49) Rankin, D. W. H.; Robertson, A. Electron-diffraction determination of molecular-structures of silyl-manganese pentacarbonyl and germyl-manganese pentacarbonyl in gas-phase. *J. Organomet. Chem.* **1975,** *85*, 225-235.

(50) Rankin, D. W. H.; Robertson, A. Gas-phase molecular-structures of methyl-rhenium, silyl-rhenium and germyl-rhenium pentacarbonyl, determined by electron-diffraction. *J. Organomet. Chem.* **1976,** *105*, 331-340.

(51) Rankin, D. W. H.; Robertson, A. Electron-diffraction determination of gas-phase structure of germylcobalt tetracarbonyl. *J. Organomet. Chem.* **1976,** *104*, 179-185.

(52) Procacci, B.; Jiao, Y. Z.; Evans, M. E.; Jones, W. D.; Perutz, R. N.; Whitwood, A. C. Activation of B-H, Si-H, and C-F Bonds with Tp'Rh(PMe_3) complexes: kinetics, mechanism, and selectivity. *J. Am. Chem. Soc.* **2015,** *137*, 1258-1272.

(53) Nolan, S. P.; Belderrain, T. R.; Grubbs, R. H. Convenient synthesis of ruthenium(II) dihydride phosphine complexes $Ru(H)_2(PP)_2$ and $Ru(H)_2(PR_3)_x$ (x = 3 and 4). *Organometallics* **1997,** *16*, 5569-5571.

(54) *Inorganic Experiments*; 3rd ed.; Woollins, J. D., Ed.; Wiley-VCH, 2009.

(55) Dransfield, T. A.; Nazir, R.; Perutz, R. N.; Whitwood, A. C. Liquid injection field desorption/ionization of transition metal fluoride complexes. *J. Fluorine Chem.* **2010,** *131*, 1213-1217.

(56) Linden, H. B. Liquid injection field desorption ionization: a new tool for soft ionization of samples including air-sensitive catalysts and non-polar hydrocarbons. *Eur. J. Mass Spectrom.* **2004,** *10*, 459-468.

(57) Gross, J. H.; Nieth, N.; Linden, H. B.; Blumbach, U.; Richter, F. J.; Tauchert, M. E.; Tompers, R.; Hofmann, P. Liquid injection field desorption/ionization of reactive transition metal complexes. *Anal. Bioanal. Chem.* **2006,** *386*, 52-58.

(58) Gross, J. H. Liquid injection field desorption/ionization-mass spectrometry of ionic liquids. *J. Am. Soc. Mass Spectrom.* **2007,** *18*, 2254-2262.

(59) Procacci, B.; Duckett, S. B.; George, M. W.; Hanson-Heine, M. W. D.; Horvath, R.; Perutz, R. N.; Sun, X. Z.; Vuong, K. Q.; Welch, J. A. Competing pathways in the photochemistry of $Ru(H)_2(CO)(PPh_3)_3$. *Organometallics* **2018,** *37*, 855-868.

(60) CrysAlisPro; Rigaku Oxford Diffraction Ltd Version 1.171.38.46 ed.

(61) Dolomanov, O. V.; Bourhis, L. J.; Gildea, R. J.; Howard, J. A. K.; Puschmann, H. OLEX2: a complete structure solution, refinement and analysis program. *J. Appl. Crystallogr.* **2009,** *42*, 339-341.

(62) Sheldrick, G. M. A short history of SHELX. *Acta Crystallographica Section A* **2008,** *64*, 112-122.

(63) Becke, A. D. Density-functional thermochemistry .3. The role of exact exchange. *J. Chem. Phys.* **1993,** *98*, 5648-5652.

(64) Grimme, S.; Ehrlich, S.; Goerigk, L. Effect of the damping function in dispersion corrected density functional theory. *J. Comput. Chem.* **2011,** *32*, 1456-1465.

(65) Gaussian 09, see Supporting Information

(66) Andrae, D.; Haussermann, U.; Dolg, M.; Stoll, H.; Preuss, H. Energy-adjusted ab initio pseudopotentials for the 2nd and 3rd row transition-elements. *Theor. Chim. Acta* **1990,** *77*, 123-141.

(67) Bergner, A.; Dolg, M.; Küchle, W.; Stoll, H.; Preuss, H. Ab-Initio energy-adjusted pseudopotentials for elements of groups 13-17. *Mol. Phys.* **1993,** *80*, 1431-1441.

(68) Ehlers, A. W.; Böhme, M.; Dapprich, S.; Gobbi, A.; Höllwarth, A.; Jonas, V.; Köhler, K. F.; Stegmann, R.; Veldkamp, A.; Frenking, G. A set of f-polarization functions for pseudo-potential basis-sets of the transition-metals Sc-Cu, Y-Ag and La-Au. *Chem. Phys. Lett.* **1993,** *208*, 111-114.

(69) Höllwarth, A.; Böhme, M.; Dapprich, S.; Ehlers, A. W.; Gobbi, A.; Jonas, V.; Köhler, K. F.; Stegmann, R.; Veldkamp, A.; Frenking, G. A set of d-polarization functions for pseudo-potential basis-sets of the main-group elements Al-Bi and f-type polarization functions for Zn, Cd, Hg. *Chem. Phys. Lett.* **1993,** *208*, 237-240.

(70) Harihara, P. C.; Pople, J. A. Influence of polarization functions on molecular-orbital hydrogenation energies. *Theor. Chim. Acta* **1973,** *28*, 213-222.

(71) Castel, A.; Riviere, P.; Satge, J.; Ko, H. Y. New (diarylgermyl)lithiums. *Organometallics* **1990,** *9*, 205-210.

Table of Contents Graphic